LUND UNIVERSITY

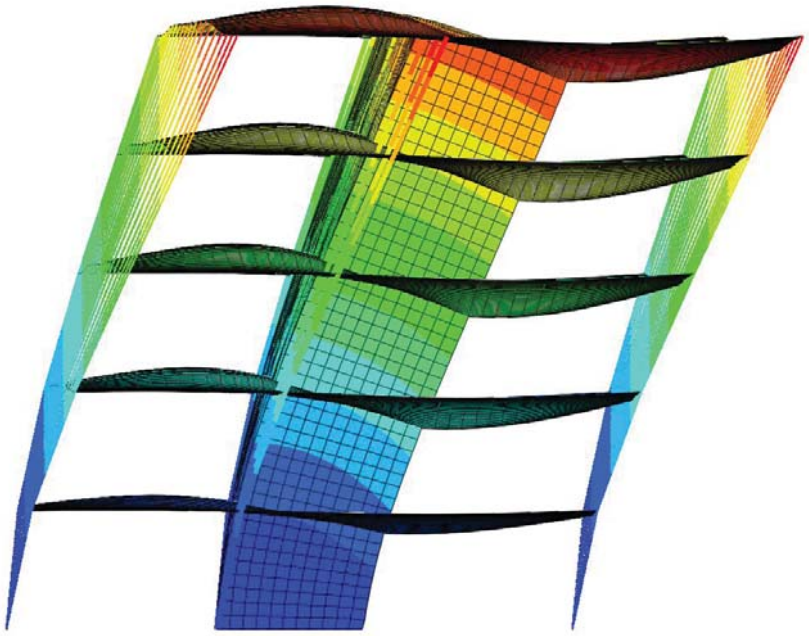

EVALUATION OF SEISMIC ACTION IN SWEDEN USING THE EUROPEAN SEISMIC HAZARD MODEL

ERIK LARSSON and LUCAS MAGNUSSON

Structural Mechanics

Master's Dissertation

DEPARTMENT OF CONSTRUCTION SCIENCES

DIVISION OF STRUCTURAL MECHANICS

ISRN LUTVDG/TVSM--17/5226--SE (1-77) | ISSN 0281-6679

MASTER'S DISSERTATION

EVALUATION OF SEISMIC ACTION IN SWEDEN USING THE EUROPEAN SEISMIC HAZARD MODEL

ERIK LARSSON and LUCAS MAGNUSSON

Supervisors: Professor **PER-ERIK AUSTRELL**, Div. of Structural Mechanics, LTH
and **LINUS ANDERSSON**, MSc, Scanscot Technology AB.

Examiner: Professor **KENT PERSSON**, Div. of Structural Mechanics, LTH.

Printed by Media-Tryck LU, Lund, Sweden, June 2017 *(Pl)*.

For information, address:
Division of Structural Mechanics,
Faculty of Engineering LTH, Lund University, Box 118, SE-221 00 Lund, Sweden.

Homepage: www.byggmek.lth.se

Preface

This thesis was initiated by Jan-Anders Larsson at Scanscot Technology and was carried on in cooperation with the Division of Structural Mechanics at Lund University during the spring of 2017. This will conclude our five years as civil engineering students at the Faculty of Engineering LTH.

We would like to address our sincerest gratitudes to our supervisor Linus Andersson at Scanscot Technology for the continuous support during the project. Furthermore, we want to thank all the employees at Scanscot Technology for valuable input and support, specially Jan-Anders who initiated and continued to review this thesis. We also would like to thank our second supervisor Prof. Per Erik Austrell at the Division of Structural Mechanics for his valuable help.

Finally, we would like to show our gratitude to our families, friends and fellow students that made the past years enjoyable.

Lund, June 2017

Erik Larsson

Lucas Magnusson

Abstract

In 2013 the European Seismic Hazard Model 2013 (ESHM13) was released as a result of the EU-funded project Seismic Harmonization in Europe (SHARE). This hazard model provides seismic data applicable for structural engineering for every location in Europe and Turkey that directly correlates to the seismic regulations provided by Eurocode 8. Currently, earthquake engineering according to Eurocode is not standard procedure for structures in Sweden due to the low regional seismicity. The objective of this thesis is to employ the data from ESHM13 and evaluate if there is reason to consider earthquakes in relation to building construction in Sweden. Specifically, the response from seismic loads for buildings of normal importance (e.g. apartment buildings) and building of vital importance (e.g. hospitals) were examined.

Eurocode 8 states that buildings of normal importance should be designed for an earthquake with a return period of 475 years. The way to differentiate building in terms of reliabilities in Eurocode 8 is to scale the reference seismic action for buildings of ordinary importance with a factor depending on importance class. This factor is a nationally determined parameter, and since these are absent in the Swedish annex it was shown that the recommended factor approximately correlates to an implicit return period of 1300 years for buildings of vital importance.

With the use of hazard data for Lund, modal response spectrum analyses were carried out on simple 2D models and a more complex 3D FE-model. The results were compared to static analyses on the same models using the wind load as comparative action. From parametric studies, that varies a range of levels and stiffnesses, the resulting base response was compared between wind load and seismic load. Spectra with return periods correlating to 475- and 1300-year were used. An additional case study was carried out on a five story building, comparing sectional forces in a shear wall due to seismic loads and wind loads.

The parametric studies clearly showed that the base response when using a 1300-year spectrum envelopes the base response from the wind load for almost every single parameter. In some cases, even a 475-year spectrum gives a higher response compared to the wind. Since the seismic response is mass-dependent and the wind response is surface-dependent, it was shown that the 475-year spectrum could easily envelope the wind for elongated building when analyzed in the long direction.

The comparison of the sectional forces in the case study suggests that the base response is a relevant measure when the overall response is compared for seismic load and wind load. However, it was shown that the seismic response is not necessarily largest at its base which suggests that the critical findings in the parametric study are potentially on the non-conservative side.

Keywords: SHARE, ESHM13, Modal Response Spectrum Analysis, Linear Dynamics.

Contents

1 Introduction

1.1 Background

In Sweden, the events of earthquakes are very rare and a lot of citizens will never experience it during a lifetime. Nevertheless, there are several earthquakes in Sweden every year. Usually they are of such small magnitude that they can only be measured with seismographs and not felt by humans. One of the more resent "major" earthquake happened in 2008. The earthquake was felt by many people in Skåne, but it only caused minor damage. The largest recorded earthquake in Sweden happened in 1904. This incident caused some damage to structures, chimneys fell over and cracks in walls were registered. There were no casualties associated with the incident.

When it comes to structural engineering it is regulated by the Eurocode and the Swedish authority Boverket. Boverket decides what parameters in Eurocode that should be used and which should be decided as nationally determined parameters. Because of the low seismicity nature of Sweden, Boverket has decided not to implement Eurocode 8 (Ec8), which regulates seismic design in Europe. It is only special structures that are engineered with regard to earthquakes. Nuclear facilities is one example, but the requirement is not set by Boverket. It is regulated by the Swedish Radiation Safety Authority (Strålsyddsmyndigheten).

In 2013 a new hazard model called European Seismic Hazard model 2013 (ESHM13) was released from a project called Seismic Hazard Harmonization in Europe (SHARE). The model is showing that the hazards around the west coast and southern Sweden are slightly higher than the rest of Sweden, see Figure 1. These new predictions might be of relevance for structures in Sweden. Especially structures of vital importance e.g. hospitals, fire station etc, which are vital if a major earthquake would occur.

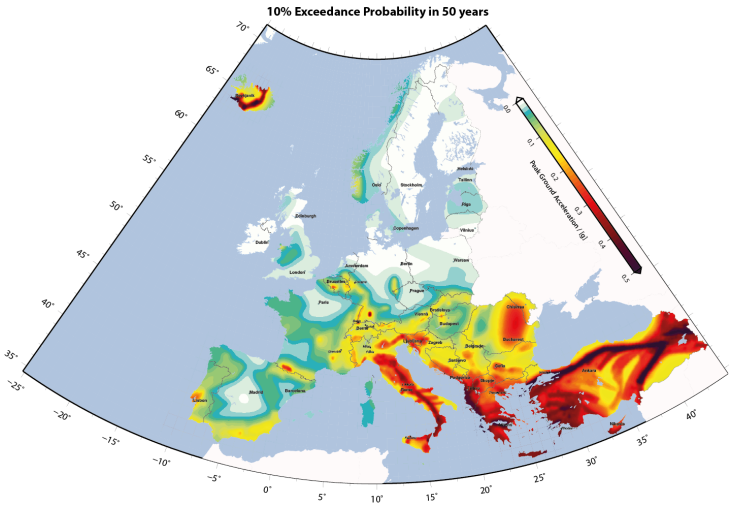

Figure 1: Hazard map over Europe according to ESHM13.

1.2 Seismic Hazard Harmonization in Europe (SHARE)

Earthquake engineering in the European countries has in the past been based on countries individual hazard assessments. With assessments performed individually by different countries the consequences are that there are often large differences in hazard levels along country borders. In order to overcome such differences the EU funded the project "Seismic Hazard Harmonization in Europe" (SHARE), which aimed to provide a reference hazard model for Europe and Turkey that was not constrained by country borders. The result of the SHARE project is the hazard model "European Seismic Hazard Model 2013"[1].

The Eurocode 8 committee was actively involved in SHARE, through specifying required output from the project. One of the SHARE objectives was to maintain a direct connection to Eurocode 8 and its applications [2]. Furthermore, it was envisaged that the outputs were designed to anticipate future revisions to the code [3].

The project documentation is available at SHARE's website (www.share-eu.org).

1.2.1 European Seismic Hazard Model 2013 (ESHM13)

As previously stated the model ESHM13 is a result of the SHARE-project. When developing ESHM13 a lot of effort was given to transparently document and making data, results and methods available to the public. Through the European Facility for Earthquake Hazard and Risk (www.efehr.org) all this information can be retrieved. The website provides users to obtain hazard assessments for every location all over Europe and Turkey.

1.3 Objective

The purpose of this paper is to evaluate the predictions from ESHM13 in southern Sweden, whether these "new" possible earthquakes could generate forces that are of significance when compared to wind loads. Since the main source of horizontal loads on buildings today are wind loads, and in most cases are what determines the capacity and geometry of a structures stabilizing system, it is considered to be a relevant measure to compare.

The comparison between seismic action and wind action are made within the scope of a design situation. This means the loads are designed according to Eurocode, however, since Eurocode 8 is not implemented in Sweden guidelines from the SHARE project are used to interpret the code.

This paper only presents an investigation of the load effects. The capacities of structures in relation to the loads are not evaluated for several reasons:

- Ductile behavior of structures may or may not be accounted for in seismic design. This is however highly dependent on the design of the structure itself and it is a difficult parameter to include in a general scope like this.

- As a general safety verification Eurocode 8 (clause 4.4.1 (2)) states that the ultimate limit state could be considered satisfied if the total base shear force due to a seismic design situation is less than that due to the other relevant action combinations for which the building is designed on the basis of a linear elastic analysis [4].
- The latter is only sufficient for low-dissipative structures, which is reasonable for most structures in Sweden as there are no "engineered" ductility in general since Eurocode 8 is not implemented.

Based on these points, the base shear force will be compared for several models within the scope of linear elastic analysis. It will be investigated whether or not the ultimate limit state could be considered satisfied without further adoption of design rules according to the writings in Eurocode 8. This is not necessarily conclusions equivalent to collapse or no collapse, but from a design stand point it could challenge the absence of seismic design in Sweden.

The objective is to find general properties of structures that can be considered critical to seismic action. It will be investigated whether the seimic action in Sweden can be treated as a designing load case if Eurocode 8 and the hazard levels from ESHM13/SHARE were to be implemented. The base shear force is investigated through parametric studies of two-dimensional beam models and complemented with a similar study of a three-dimensional FE-model in order to validate the beam models.

Furthermore it will be illustrated how seismic forces can be distributed through out a building by doing a case study of a building that is considered to be critical. This is to show how relevant the total base shear force is in relation to local section forces and moments in higher stories.

2 Theory

In this study the analyses are made using modal response spectrum analysis (RSA). In order to perform such an analysis the first step is to identify a hazard correlated to a specific probability of exceedance, which is done using a probabilistic seismic hazard assessment. The hazard is described as peak accelerations corresponding to a frequency of a single degree of freedom system (SDOF-system) and a probability of exceedance. Using these accelerations, a spectrum can be created usually plotted against natural periods. When the modal analysis is performed an acceleration for each natural period is retrieved from the spectrum. The result from the modal analysis will give an approximated solution to what the structures response will be when its exposed to an earthquake. These concepts and the connected theory will be explained in the following sections. A section describing the wind load is also found in the following sections. This will become relevant to the evaluation of the analysis at the end of the study.

2.1 Probabilistic Seismic Hazard Assessment (PSHA)

To make one able to analyze structures for seismic loads a model/prediction of possible earthquakes is necessary. Probabilistic Seismic Hazard Assessment (PSHA) is the most common method of addressing the seismic threat in civil engineering. The method is based on earthquake catalogues that covers data from past earthquakes in a specific region. Due to the fact that the earthquake catalogues usually covers a relatively short time period it is necessary to make some predictions based on regional geological and seismological data. With the data and predictions combined a source zone model, that is calibrated to the regions specific properties (e.g distance from faults, types of earthquakes etc.) can be created, which is the foundation of a PSHA [5].

The output from the assessment is the probability that a certain ground motion intensity measure (e.g. peak ground acceleration) will exceed a threshold limit during a certain time period. Hence, the magnitude of the intensity measure is often corresponding to a "return period". In other words, the return period controls the seismic action and the choice of return period depends on the target-reliability of the structure.

2.1.1 Return Period

If the number of events where the magnitude exceeds the threshold limit during a time period T_L is assumed to be Poisson distributed, the relationship between the return period T_R and the probability of exceedance P can be calculated as:

$$T_R = -T_L / \ln(1 - P) \tag{1}$$

Within earthquake engineering the time period of reference T_L is normally 50 years thus the return period T_R corresponds to a specific probability of exceedance in 50 years.

As an example, an earthquake with a magnitude m that has a 10 % probability of exceedance a threshold M during 50 years has an approximate return period of:

$$T_R = -50/\ln(1 - 0.10) \approx 475 \text{ years} \tag{2}$$

In Eurocode 8 (Ec8) the return period is a so called nationally determined parameter (NDP), the recommended value for structures of ordinary importance is however 475 years, i.e. 10% probability of exceedance in 50 years [4]. This recommendation is made with regard to design for the Ultimate Limit State (ULS).

2.1.2 Return periods in relation to wind loads

Variable loads in different parts of Eurocode are normally designed for a return period of 50 years, i.e. 2% probability of exceedance in 1 year. This is also used for wind loads. The wind load can be scaled with the factor c_{prob} to obtain the characteristic wind load for different return periods [6]. It is used by directly multiplying it with the basic wind velocity (v_b). With Equation 3 the scale factor can be calculated using K, which is a shape parameter depending on the coefficient of variation of the extreme-value distribution, p, which is the desired probability of exceedance in one year and n, which is the exponent. The values of K and n are NDPs and they are set to 0.2 and 0.5 respectively. Figure 2 shows how c_{prob} varies for different return periods.

$$c_{prob} = \left(\frac{1 - K \cdot \ln(-\ln(1 - p))}{1 - K \cdot \ln(-\ln(0.98))} \right)^n \tag{3}$$

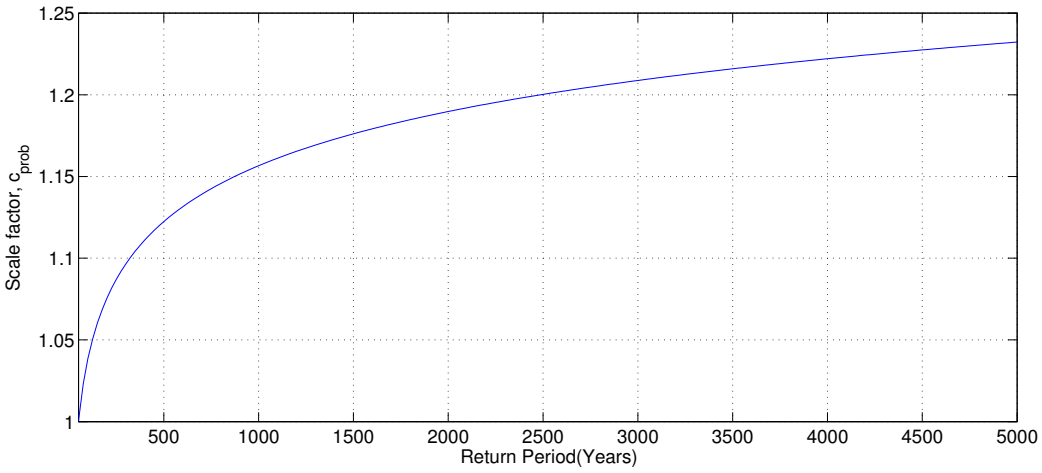

Figure 2: Plot of scale factor c_{prob} and correlated return periods.

The values of c_{prob} range from 1.0 for a return period of 50 years to approximately 1.23 for a return period of 5000 years, see Figure 2. This goes to show that the wind load

does not statistically become significantly larger than the characteristic value. The same principle is not applicable for an earthquake with a return period of 475 years, which will be shown in this paper becomes significantly larger for longer return periods.

2.2 Representations of Seismic Action in Civil Engineering

Engineers need a meaningful representation of ground motion in their definitions of seismic action and thus common outputs from PSHA are expected accelerations in terms of ground values or spectrum over a range of frequencies. Intensity measures of displacements and velocities can also be obtained from PSHA, however this paper focuses on accelerations as these correlates to seismic forces which are to be evaluated.

Some of the most common representations of seismic action are presented in the sections below.

2.2.1 Peak Ground Acceleration (PGA)

Peak ground acceleration (PGA) is the maximum acceleration in a point on the ground during an earthquake. From PSHA the PGA can be estimated based on the probability of exceedance (PE). Figure 3 shows the PE as a function of PGA at a specific site (Lund, Sweden)[7].

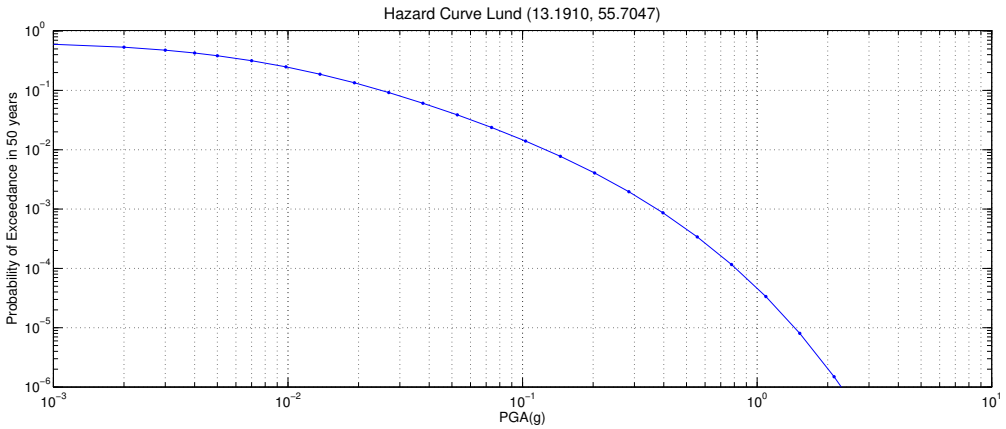

Figure 3: Probability of exceedance as a function of PGA.

There is one significant weakness with the use of PGA. If the PGA-value increases it does not directly correlate with an increase of structural damage. The reason is that the response in a structure subjected to dynamic loading is dependent on the natural frequency/period of the structure and PGA does not provide any information about the frequencies of the ground motion. PGA is however a commonly used parameter in building codes, e.g. Eurocode 8, as a basis for shaping design spectrum [4]. This will be further explained in Section 3.2.

2.2.2 Uniform Hazard Spectrum (UHS)

The peak displacement $\max(|u(t)|)$ in a SDOF-system with a frequency ω_n can be calculated from a ground motion or as an envelope from several ground motions. This is known as spectral displacement, SD_n.

$$SD_n \equiv \max(|u(t)|) \tag{4}$$

As such, the peak displacements can be represented in a spectrum for a range of SDOF-systems with different frequencies ω_n. The spectral velocities SV_n and accelerations SA_n are given by:

$$SV_n = \omega_n SD_n \tag{5}$$

$$SA_n = \omega_n^2 SD_n \tag{6}$$

These quantities are sometimes referred to as *pseudeo-velocity* and *pseudeo-acceleration*. The reason is they are not actually the peak velocities and accelerations. The spectral velocity correlates to a kinetic energy that is exactly the same as the maximum strain energy obtained from the spectral displacements. Assuming the velocity V is related to the displacements D as $V = \omega_n D$, the strain energy is given by

$$E = \frac{kD^2}{2} = \frac{k(V\omega_n)^2}{2} = \frac{mV^2}{2} \tag{7}$$

where the right side of the equation is the expression for kinetic energy. In other words, V can only be interpreted as peak velocity if there is a continuous transfer between strain energy and kinetic energy. Since the velocity spectrum is not used in this paper, there is no reason to analyze the implications of this approximation in depth. However the acceleration spectrum is, which similarly can be derived from the largest forces in the system. If the acceleration is related to the displacements as $A = \omega_n^2 D$, the force (base shear force) is calculated as

$$f = kD = m\omega_n^2 D = mA \tag{8}$$

As such, the pseudo-acceleration actually provides the true forces of the system [8]. From here on there are no distinctions made between pseudo-acceleration and *true* spectral accelerations, as the pseudo-acceleration provides the *true* forces.

The magnitude of a specific SA_n can be expressed in terms of probability of exceedance. With extractions from a range of SA_n a Uniform Hazard Spectrum can be assembled. In Figure 4 it is shown how a UHS assembled. In the upper part of the figure hazard spectra of natural periods of 0.5 respectively 1.0 seconds are plotted. From these curves, values of SA_n with a probability of exceedance of 10% in 50 years are chosen and then transfered

to a UHS (lower part of the figure). One of the benefits of a UHS is that it considers the specific characteristics of a region. Dependent on what types of earthquakes (e.g. near fault or far fault earthquakes) are common in a region different periods of SA_n will be more or less excited.

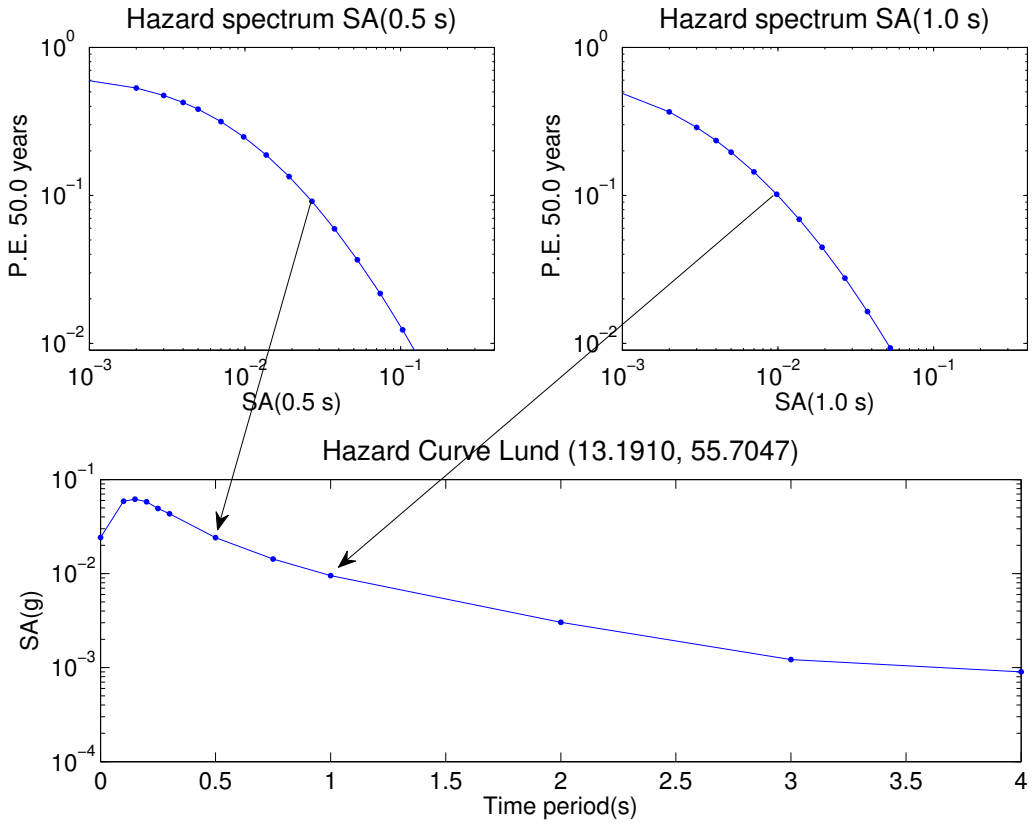

Figure 4: Explanation of UHS from individual Hazard spectra.

The spectral ordinates, SA(1.0s), SA(2.0s) etcetera, are estimations of the *mean* peak response at the site a certain distance from the earthquake source. Thus, the UHS for e.g. 475 years is not an envelope of a "worst considered earthquake" during 475 years as it not intended to envelope all earthquakes at all spectral periods during that time period. As an example, recorded spectral accelerations at 1 second was recorded for the 1999 Chi-Chi earthquake in Taiwan at different sites as shown in Figure 5. At a given distance from the source, different sites experienced different ground motions resulting in a wide range of spectral ordinates [9].

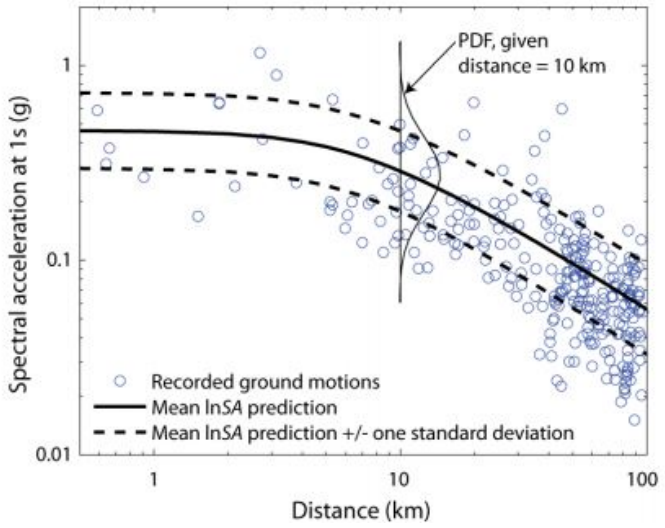

Figure 5: Observed spectral acceleration values from the 1999 Chi-Chi, Taiwan earthquake [9].

The spectral ordinate that could be used to predict the hazard at a site is the mean value of all spectral ordinates at a given distance from the source. Consequently, the UHS could also be expressed as $+/-$ X number of standard deviations for more or less conservative approaches. In this paper, the UHS referrers to the mean spectrum.

Each spectral ordinate is also a function of the damping ratio ζ_n for each mode. Normally the values of each spectral ordinate are given for a fixed value of ζ_n and these values can be re-calculated for other damping values. The spectral ordinates from ESHM13 are given for SDOF-systems with 5% damping.

2.2.3 Design spectrum

The design spectrum has a central role in earthquake engineering and the intention of constructing a design spectrum is to characterize the effects of ground motion on buildings in a practical way. The design spectrum is essentially an idealized UHS that is derived from parameterized seismic conditions. It is comprised of different branches, where SDOF-systems with different natural periods T_n are expected to reach constant peak values of either accelerations, velocities or displacements within each branch. Most notably, the largest acceleration is expressed as a constant branch over a wide range of periods as seen in Figure 6.

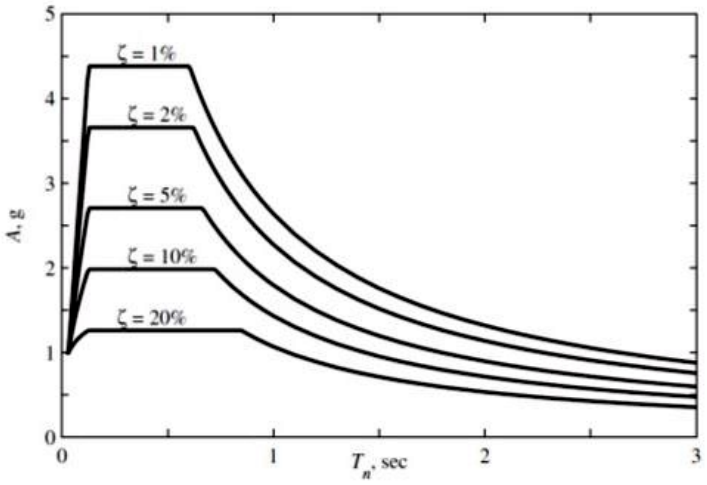

Figure 6: Design spectrum containing spectral accelerations A as a function of natural periods T_n.

Various damping ratios can be used which reflect on the variety of different building structural properties. In Figure 6 a design spectrum is presented, representing peak spectral accelerations ($A(T_n, \zeta) \equiv \max|\ddot{u}(t, T_n, \zeta)|$) for different values of ζ. Other peak responses that could be used in a similar spectrum is peak velocity ($V(T_n, \zeta) \equiv \max|\dot{u}(t, T_n, \zeta)|$) or peak displacements ($D(T_n, \zeta) \equiv \max|u(t, T_n, \zeta)|$) [8].

2.3 Modal response spectrum analysis

The most intuitive method to apply an earthquake load is perhaps to expose a structure to a simulated ground motion. Recorded time series from different sites can be scaled to fit a design spectrum for a specific site of interest and then be used in such analysis. Synthetic time series can also be used for the same purpose. A more common method in a design situation is however, and required by Eurocode 8, to apply the force directly from the design spectrum without involving time series. This method is known as *Modal response spectrum analysis* and it is possible since the pseudo response, e.g. spectral acceleration, for all modes and earthquakes are covered by the design spectrum.

A system subjected to an earthquake load responds very close with the natural frequencies of the system. The key notion here is that each frequency is linked to a certain mode shape and inertia forces are required to produce it. Each mode distributes the masses differently and since the acceleration is known for each mode (from the design spectrum) the inertia forces can be found by solving the eigenfrequencies/periods f_n/T_n of the system. Each mode contribute to the response and how much depends on mode shape $\boldsymbol{\phi}(T_n)$ and spectral acceleration $Sa(T_n, \zeta_n)$.

The theory presented in this section covers the essential information needed to understand how a modal response spectrum analysis is performed. Necessary assumptions are required and a solution to the most obvious drawback with loosing the time aspect in a spectrum

analysis is presented. The theory can be found in, although slightly differently formulated here, *Dynamics of Structures* by Anil K. Chopra [8].

2.3.1 Effective earthquake force

In order to explain the method behind modal response analysis it is useful to understand the general concept behind the equation of motion in relation to earthquakes. Since the excitation of structures, represented in this case by a multi degree of freedom (MDOF) system, during an earthquake is induced through displacement of the ground it is necessary to be able to express the relative displacement of the structure, see Figure 7. The MDOF system is composed by $j = 1$ to N masses (representing stories). The total displacement of the system is denoted by u_j^t. To describe the total displacement, the ground displacement, u_g, and the relative displacement, u_j, is used, see Equation 9.

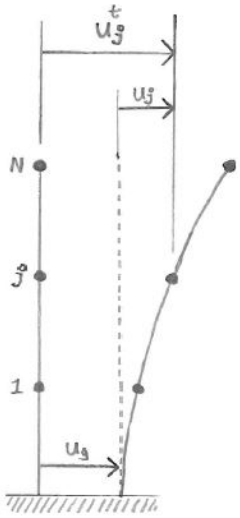

Figure 7: Illustration of relative displacement.

$$u_j^t(t) = u_g(t) + u_j(t) \tag{9}$$

Equation 9 can be written on matrix form as

$$\boldsymbol{u}^t(t) = u_g(t)\boldsymbol{\iota} + \boldsymbol{u}(t) \tag{10}$$

where the vector $\boldsymbol{\iota}$ in Equation 10 is an influence vector describing the displacement of the systems N masses when applying a static displacement of a unit ground displacement. Each element in $\boldsymbol{\iota}$ equals the projection of the unit ground displacement onto the corresponding degree of freedom. Each element is equal to 1 if the unit ground displacement is parallel to the corresponding degree of freedom in $\boldsymbol{\iota}$ as seen in Figure 8.

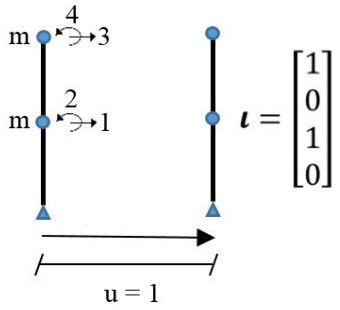

Figure 8: Visualization of influence vector $\boldsymbol{\iota}$.

The equation of motion is in matrix format given in Equation 11.

$$\boldsymbol{m\ddot{u}} + \boldsymbol{c\dot{u}} + \boldsymbol{ku} = \boldsymbol{p}(t) \tag{11}$$

The equation consists of four parts. $\boldsymbol{m\ddot{u}}$ is the mass matrix and the acceleration vector which represents the inertia forces of the system. $\boldsymbol{c\dot{u}}$ is the damping matrix and the velocity vector which represents the damping forces of the system. $\boldsymbol{ku}$ is the stiffness matrix and the displacement vector which represents the elastic forces in the system. The vector $\boldsymbol{p}(t)$ is the load vector which contains the external forces. When analyzing earthquakes no external loads will be applied and the load vector is zero, i.e. $\boldsymbol{p}(t) = \boldsymbol{0}$.

Elastic and damping forces are only dependent on the relative displacement $\boldsymbol{u}$, since the displacement of the ground resembles a rigid body motion of the whole structure. However the inertia forces are dependent on the total acceleration, $\ddot{\boldsymbol{u}}^t$, of the masses. If the relation in equation 10 is differentiated two times an expression for the total acceleration is generated. If this relationship is used in equation 11 with $\boldsymbol{p}(t) = 0$ the following equation is given:

$$\boldsymbol{m\ddot{u}} + \boldsymbol{c\dot{u}} + \boldsymbol{ku} = -\boldsymbol{m\iota}\ddot{u}_g(t) \tag{12}$$

If equation 11 and 12 are compared one can see that they are the same with an exception for the load vector. The ground motion can therefore be expressed as a load vector described as effective earthquake force:

$$\boldsymbol{p}_{eff}(t) = -\boldsymbol{m\iota}\ddot{u}_g(t) \tag{13}$$

2.3.2 Eigenvalue problem

Since analyzes made in this paper are made within the scope of modal analysis, the natural frequencies have to be calculated. To be able to retrieve the natural frequencies, ω_n, and the corresponding mode shape vector, ϕ_n, of a system, the following equation(called the matrix eigenvalue problem) needs to be solved:

$$\boldsymbol{k}\phi_n = \omega_n^2 \boldsymbol{m}\phi_n \tag{14}$$

The equation will only supply the solution without consideration of damping, hence a damped system is determined by the complex eigenvalue problem. Both matrices $\boldsymbol{k}$ and $\boldsymbol{m}$ are known and what to be determined is the scalar ω_n^2 and its correlated vector ϕ_n.

$$[\boldsymbol{k} - \omega_n^2 \boldsymbol{m}]\boldsymbol{\phi}_n = 0 \tag{15}$$

With equation 14 rewritten as above its intuitive that one solution to the problem is $\phi_n = 0$. This is the trivial solution which implies that the system is exposed to no motion. The non trivial solution is given if the following equation is fulfilled:

$$\det[\boldsymbol{k} - \omega_n^2 \boldsymbol{m}] = 0 \tag{16}$$

If a system has N elements, when expanding the determinant a polynomial of order N in ω_n^2 is given. The polynomial has N number of real and positive roots for ω_n. The N roots describing the natural frequency ω_n is sorted in an increasing manner$(\omega_1, \omega_2, ..., \omega_N)$. By using each natural frequency ω_n, N individual mode shape vectors ϕ_n are produced when solving equation 15. The shape vector does not contain information about the magnitude of the displacements. It only contains the relative displacement.

2.3.3 K- and M- orthogonality of modes

The mode vectors orthogonality is an important property that is used when doing a modal expansion. The following condition needs to be fulfilled, when $\omega_n \neq \omega_r$. The mode vectors are orthogonal with $\boldsymbol{k}$ and $\boldsymbol{m}$ according to equation 17.

$$\phi_n^T \boldsymbol{k} \phi_r = 0 \qquad \phi_n^T \boldsymbol{m} \phi_r = 0 \tag{17}$$

In order to prove this relationship, equation 14 is premultiplied with ϕ_r^T (the transpose of ϕ_r). The equation is satisfied for nth natural frequency and mode which gives,

$$\phi_r^T \boldsymbol{k} \phi_n = \omega_n^2 \phi_r^T \boldsymbol{m} \phi_n \tag{18}$$

If the same procedure is done for the rth natural frequency and mode, but premultiplying with ϕ_n^T, this gives,

$$\phi_n^T \boldsymbol{k} \phi_r = \omega_r^2 \phi_n^T \boldsymbol{m} \phi_r \tag{19}$$

The transpose of the matrix on the left side of equation 18 will equal the transpose of the matrix on the right side of the equation, thus

$$\phi_n^T \boldsymbol{k} \phi_r = \omega_n^2 \phi_n^T \boldsymbol{m} \phi_r \tag{20}$$

Here the symmetry property of the stiffness and mass matrix has been utilized. If equation 19 is subtracted from equation 20 the following equation is given,

$$(\omega_n^2 - \omega_r^2) \phi_n^T \boldsymbol{m} \phi_r = 0 \tag{21}$$

This shows that the equation to the right in equation 17 is true when $\omega_n^2 \neq \omega_r^2$. For systems with only positive natural frequencies this implies that $\omega_n \neq \omega_r$. By substituting the right part of equation 17 in equation 19 it is shown that the left part of equation 17 is true when $\omega_n \neq \omega_r$.

2.3.4 Modal expansion of displacements

The mode vectors ϕ_r form an orthogonal base in which any displacement $\boldsymbol{u}$(t) can be expressed as linear combination of the mode vectors as shown in Equation 22.

$$\boldsymbol{u}(t) = \sum_{r=1}^{N} \boldsymbol{\phi}_r q_r(t) \tag{22}$$

q_r(t) are time dependent scalars and are known as *modal coordinates*. Derivation once and twice of Equation 22 yields after insertion in the equation of motion:

$$\sum_{r=1}^{N} \boldsymbol{m} \boldsymbol{\phi}_r \ddot{q}_r(t) + \sum_{r=1}^{N} \boldsymbol{c} \boldsymbol{\phi}_r \dot{q}_r(t) + \sum_{r=1}^{N} \boldsymbol{k} \boldsymbol{\phi}_r q_r(t) = \boldsymbol{p}_{eff}(t) \tag{23}$$

The same equation can also be multiplied with $\boldsymbol{\phi}_n^T$ on the left side of each term as shown in Equation 24.

$$\sum_{r=1}^{N} \boldsymbol{\phi}_n^T \boldsymbol{m} \boldsymbol{\phi}_r \ddot{q}_r(t) + \sum_{r=1}^{N} \boldsymbol{\phi}_n^T \boldsymbol{c} \boldsymbol{\phi}_r \dot{q}_r(t) + \sum_{r=1}^{N} \boldsymbol{\phi}_n^T \boldsymbol{k} \boldsymbol{\phi}_r q_r(t) = \boldsymbol{\phi}_n^T \boldsymbol{p}_{eff}(t) \tag{24}$$

For $n \neq r$ the terms $\boldsymbol{\phi}_n^T \boldsymbol{m} \boldsymbol{\phi}_r$ and $\boldsymbol{\phi}_n^T \boldsymbol{k} \boldsymbol{\phi}_r$ equals zero due to orthogonal properties of modes with distinct frequencies ($\omega_n \neq \omega_r$). For $n = r$ the terms become scalars $M_n = \boldsymbol{\phi}_n^T \boldsymbol{m} \boldsymbol{\phi}_n$ and $K_n = \boldsymbol{\phi}_n^T \boldsymbol{k} \boldsymbol{\phi}_n$. The equation can be rewritten as:

$$M_n \ddot{q}_n(t) + \sum_{r=1}^{N} C_{nr} \dot{q}_r(t) + K_n q_n(t) = P_{n,eff}(t) \tag{25}$$

where C_{nr} and $P_{n,eff}$ are defined as:

$$C_{nr} = \boldsymbol{\phi}_n^T \boldsymbol{c} \boldsymbol{\phi}_r \qquad P_{n,eff} = \boldsymbol{\phi}_n^T \boldsymbol{p}_{eff} \tag{26}$$

For $n = 1$ to $n = N$ Equation 25 yields a set of N coupled equations. On matrix form these can be written as:

$$\boldsymbol{M}\ddot{\boldsymbol{q}} + \boldsymbol{C}\dot{\boldsymbol{q}} + \boldsymbol{K}\boldsymbol{q} = \boldsymbol{P}_{eff} \tag{27}$$

$\boldsymbol{M}$ and $\boldsymbol{K}$ are diagonal but $\boldsymbol{C}$ may or may not be. The equations are coupled since the modal velocity $\dot{q}_r$ for $r = 1$ to N is represented in every equation n. However, if classical damping is assumed $\boldsymbol{C}$ becomes diagonal, i.e. $C_{nr} = 0$ and $C_{nn} = \boldsymbol{\phi}_n^T \boldsymbol{c} \boldsymbol{\phi}_n$. This uncouples all equations in (27) which is a fundamental assumption for the rest of this paper. Each equation in (27) are then given by:

$$M_n\ddot{q}_n(t) + C_n\dot{q}_n(t) + K_n q_n(t) = P_{n,eff}(t) \tag{28}$$

Dividing the equation with M_n yields:

$$\ddot{q}_n(t) + 2\zeta_n\omega_n\dot{q}_n(t) + \omega_n^2 q_n(t) = \frac{P_{n,eff}(t)}{M_n} \tag{29}$$

where ζ_n is the damping ratio for mode n. The damping ratio is defined as:

$$\zeta_n = \frac{C_n}{2M_n\omega_n} \tag{30}$$

which explains the transition from Equation 28 to 29. The denominator $2M_n\omega_n$ is the smallest damping value C_n can have that prevents oscillation of mode n completely. Equation 30 is not explicitly implemented in this paper, instead mode n is assigned a value ζ_n. In other words, a building is assumed to have a certain damping. In this case, all modes are assumed to have a damping ratio $\zeta_n = 0.05$.

2.3.5 Modal expansion of earthquake forces

The effective earthquake force is given by:

$$\boldsymbol{p}_{eff}(t) = -\boldsymbol{m}\boldsymbol{\iota}\ddot{u}_g(t) \tag{31}$$

The influence vector $\boldsymbol{\iota}$ can be expressed as a combination of mode vectors as shown in the equation below.

$$\boldsymbol{\iota} = \sum_{n=1}^{N} \Gamma_n \boldsymbol{\phi}_n \tag{32}$$

Γ_n is a scalar with different values for each mode n. It follows that

$$\boldsymbol{m}\boldsymbol{\iota} = \sum_{n=1}^{N} \boldsymbol{s}_n = \sum_{n=1}^{N} \Gamma_n \boldsymbol{m}\boldsymbol{\phi}_n \tag{33}$$

where $\boldsymbol{s}_n = \Gamma_n \boldsymbol{m}\boldsymbol{\phi}_n$ is the inertia distribution of mode n. Figure 9 shows the expansion of $\boldsymbol{m}\boldsymbol{\iota} = [2m; m]$ for a two story frame with $\boldsymbol{\phi}_1 = [\frac{1}{2}; 1]$ and $\boldsymbol{\phi}_2 = [-1; 1]$.

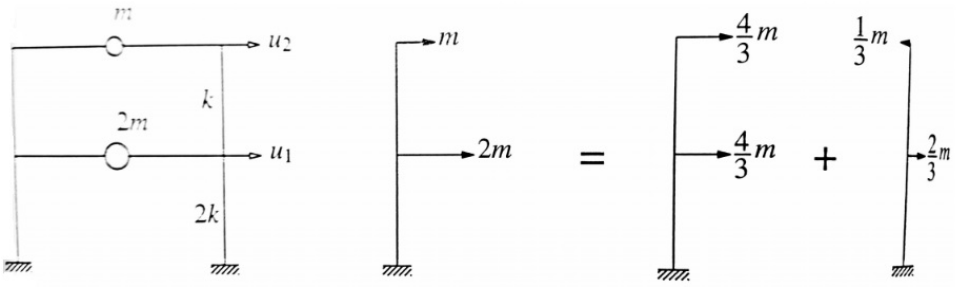

Figure 9: Illustration showing modal expansion of $\boldsymbol{m}\boldsymbol{\iota}$.

In this case the values of Γ_1 and Γ_2 are $4/3$ and $-1/3$ respectively. These values can be found by multiplying both sides of Equation 33 with $\boldsymbol{\phi}_r^T$ in order to obtain

$$\boldsymbol{\phi}_r^T \boldsymbol{m}\boldsymbol{\iota} = \Gamma_r \boldsymbol{\phi}_r^T \boldsymbol{m}\boldsymbol{\phi}_r \tag{34}$$

by using orthogonal properties of the mode vectors on the right side of the equation. For convenience the subscript r is changed back to n and an expression for Γ_n is found:

$$\Gamma_n = \frac{\boldsymbol{\phi}_n^T \boldsymbol{m}\boldsymbol{\iota}}{\boldsymbol{\phi}_n^T \boldsymbol{m}\boldsymbol{\phi}_n} = \frac{L_n}{M_n} \tag{35}$$

Recalling the equation of motion:

$$\ddot{q}_n(t) + 2\zeta_n \omega_n \dot{q}_n(t) + \omega_n^2 q_n(t) = \frac{P_{n,eff}(t)}{M_n} \tag{36}$$

where the effective modal force is given by:

$$P_{n,eff}(t) = \boldsymbol{\phi}_n^T \boldsymbol{p}_{eff}(t) \tag{37}$$

Combining Equation 31, 33 and 37 yields:

$$P_{n,eff}(t) = -\sum_{r=1}^{N} \Gamma_r \boldsymbol{\phi}_n^T \boldsymbol{m}\boldsymbol{\phi}_r \ddot{u}_g(t) \tag{38}$$

From orthogonality of modes the following expression is obtained:

$$P_{n,eff} = -\Gamma_n M_n \ddot{u}_g \tag{39}$$

Insertion of Equation 39 into the equation of motion gives the modal equation specialized for earthquake excitations:

$$\ddot{q}_n(t) + 2\zeta_n \omega_n \dot{q}_n(t) + \omega_n^2 q_n(t) = -\Gamma_n \ddot{u}_g(t) \tag{40}$$

2.3.6 Modal Response

The equation of motion for a SDOF system with a frequency $\omega = \omega_n$ and damping $\zeta = \zeta_n$ is given by:

$$\ddot{D}_n + 2\zeta_n\omega_n\dot{D}_n + \omega^2 D_n = -u_g(t) \tag{41}$$

where D_n is the displacements. The subscript n is used since it can be compared easily with the modal equation for a MDOF system with the same damping and frequency below.

$$\ddot{q}_n(t) + 2\zeta_n\omega_n\dot{q}_n(t) + \omega_n^2 q_n(t) = -\Gamma_n\ddot{u}_g(t) \tag{42}$$

It can be established that

$$q_n(t) = \Gamma_n D_n(t) \tag{43}$$

if $\omega = \omega_n$ and $\zeta = \zeta_n$. In other words, the modal coordinates q_n are proportional to the displacements of a SDOF system with the same damping and frequency as the nth mode of the MDOF system. Thus, the contribution of the nth mode to the nodal displacements can be calculated as:

$$\boldsymbol{u}_n(t) = \boldsymbol{\phi}_n q_n(t) = \Gamma_n\boldsymbol{\phi}_n D_n(t) \tag{44}$$

The equivalent external static forces $\boldsymbol{f}_n(t)$ required to produce $\boldsymbol{u}_n$(t) at time t is calculated as

$$\boldsymbol{f}_n(t) = \boldsymbol{k}\boldsymbol{u}_n(t) = \Gamma_n\boldsymbol{k}\boldsymbol{\phi}_n D_n(t) \tag{45}$$

Recalling the eigenvalue problem $\boldsymbol{k}\boldsymbol{\phi}_n = \omega_n^2\boldsymbol{m}\boldsymbol{\phi}_n$ and the intertia distribution $\boldsymbol{s}_n = \Gamma_n\boldsymbol{m}\boldsymbol{\phi}_n$ equation 45 can be rewritten as:

$$\boldsymbol{f}_n(t) = \boldsymbol{s}_n\omega_n^2 D_n(t) = \boldsymbol{s}_n A_n(t) \tag{46}$$

where $A_n = \omega_n^2 D_n$ is the acceleration for a SDOF system with frequency and damping ω_n respectively ζ_n. The modal response (of any quantity) $r_n(t)$ in a structure is determined by static analysis of the structure subjected to external forces $\boldsymbol{f}_n(t)$. If r_n^{st} denotes the static modal response due to a "force" $\boldsymbol{s}_n$, the modal response due to an external force $\boldsymbol{f}_n$ can be calculated as:

$$r_n(t) = r_n^{st} A_n(t) \tag{47}$$

$\boldsymbol{s}_n$ is here falsely denoted as a force as it has units of mass but the quantity satisfy $\boldsymbol{s}_n = \boldsymbol{k}\boldsymbol{u}_n^{st}$ as:

$$\boldsymbol{u}_n^{st} = \boldsymbol{k}^{-1}\boldsymbol{s}_n = \frac{\Gamma_n}{\omega_n^2}\boldsymbol{\phi}_n \tag{48}$$

and substituting $\boldsymbol{u}_n^{st}$ as r_n^{st} in Equation 47 yields

$$\boldsymbol{u}_n(t) = \frac{\Gamma_n}{\omega_n^2}\boldsymbol{\phi}_n A_n(t) = \Gamma_n\boldsymbol{\phi}_n D_n(t) \tag{49}$$

which is exactly the same as Equation 44. This goes to show that any response quantity r_n can be calculated according to Equation 47. The modal static response r_n^{st} due to a

force $\boldsymbol{s}_n$ is however calculated differently depending on response quantity.

The most straight forward static response quantity to determine is the static modal base shear force V_{bn}^{st}. For a multistory frame building with masses located at floor levels as seen in Figure 10, the static base shear is solved for equilibrium with $\boldsymbol{s}_n$.

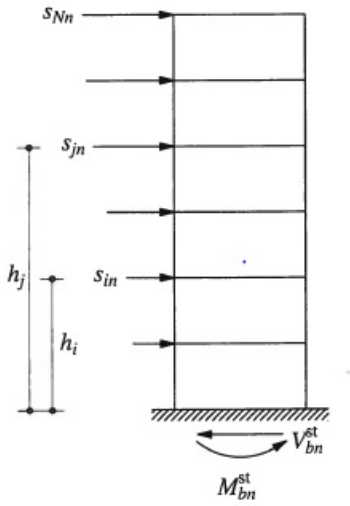

Figure 10: Illustration of modal static base shear and base moment.

The modal static base shear force can be calculated as

$$V_{bn}^{st} = \boldsymbol{s}_n^T \boldsymbol{\iota} = \Gamma_n \boldsymbol{\phi}_n^T \boldsymbol{m} \boldsymbol{\iota} = \Gamma_n L_n \tag{50}$$

where Γ_n and L_n are repeated here for a summary of the theory:

$$\Gamma_n = \frac{\boldsymbol{\phi}_n^T \boldsymbol{m} \boldsymbol{\iota}}{\boldsymbol{\phi}_n^T \boldsymbol{m} \boldsymbol{\phi}_n} = \frac{L_n}{M_n} \tag{51}$$

The modal static base shear force V_{bn}^{st} is exactly equal to the *effective modal mass*, an important concept in modal analysis. The effective modal mass is defined as

$$M_n^* = \Gamma_n L_n \tag{52}$$

A SDOF-system is 100 % effective in producing base shear force, since all inertia is transfered down to the ground. A MDOF system oscillating in mode n can however only produce a base shear force proportional to M_n^*. The contribution from the nth mode to the base shear is calculated by combining Equation 47, 50 and 52:

$$V_{bn} = M_n^* A_n(t) \tag{53}$$

The total mass of the building M_t is equal to the sum of each effective modal mass, i.e:

$$M_t = \sum_{n=1}^{N} M_n^* \tag{54}$$

2.3.7 Time independent modal analysis

The ground motion of a particular earthquake $\ddot{u}_g(t)$ can produce an acceleration $A_n(t)$ for each mode n. The peak acceleration for each mode, known as *spectral acceleration* $Sa(T_n, \zeta_n)$ is dependent on the damping and natural period of vibration of that mode, for that particular earthquake. By exposing a set of SDOF-systems with different T_n and ζ_n to a ground motion $\ddot{u}_g(t)$ the spectral acceleration for each mode n can be calculated. As an example the response spectrum for El Centro earthquake for $\zeta = 0.02$ is shown in the figure below.

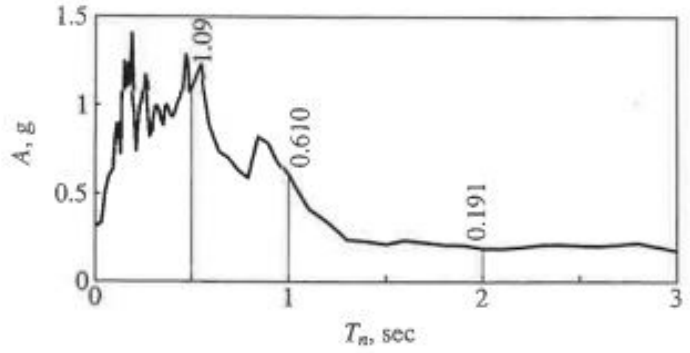

Figure 11: Response spectrum from El Centro earthquake showing the ground motion $\zeta = 0.02$.

If the response spectrum is known for a particular earthquake, the maximum response for each mode r_{no} can be calculated according to the equation below.

$$r_{no} = r_n^{st} A_{n,max} = r_n^{st} Sa(T_n, \zeta_n) \tag{55}$$

The information of which time t the response r_{no} occurs is lost thus it is unknown how r_{no} for each mode n coincide in time. There are however different methods of combining the response for each mode n, two of which are explained in the next section.

Since the scope of this project is to investigate all possible earthquakes during a certain time period one response spectrum is not enough. Instead a design spectrum is used, explained in Section 3.2, since this is an idealized envelope of all possible earthquakes. The procedure is however not changed, Equation 55 is still valid but the spectral acceleration $Sa(T_n, \zeta_n)$ is a representation of all possible earthquakes.

2.3.8 Modal combination rules (SRSS and CQC)

As described in the previous chapter the values of r_{no} $(n = 1, 2, ..., N)$ represents the peak modal responses. In general different modes reach their peak value at different time instances. If one were to sum the absolute values of each modal contribution, it would be equivalent to say that the peak response for each mode coincide in time. This is usually

considered to be too conservative. There are several modal combination rules that can be used instead, of which two are presented here and preferred by Ec8 [4].

Square Root of Sum of Squares (SRSS) is a modal combination rule accepted for structures with well separated frequencies. The total response is estimated by summing the square roots of the modal responses as shown in equation 56.

$$r_o \simeq \left(\sum_{n=1}^{N} r_{no}^2 \right)^{1/2} \tag{56}$$

If the modes are closely spaced in frequencies the *Complete Quadratic Combination* CQC method is preferred as it takes the correlation of close frequencies into account. The CQC combination rule is presented in Equation 57 below.

$$r_o \simeq \left(\sum_{n=1}^{N} r_{no}^2 + \sum_{i=1}^{N} \sum_{n=1}^{N} \rho_{in} r_{io} r_{no} \right)^{1/2} \quad \text{, where} \quad i \neq n \tag{57}$$

The correlation factor ρ_{in} depends on the frequency ratio $\beta_{in} = \omega_i/\omega_n$ and the modal damping ζ , assuming $\zeta = \zeta_i = \zeta_n$, as:

$$\rho_{in} = \frac{8\zeta^2(1+\beta_{in})\beta_{in}^{3/2}}{(1-\beta_{in}^2)^2 + 4\zeta^2\beta_{in}(1+\beta_{in})^2} \tag{58}$$

The correlation factor can vary between 0 and 1 and note for $\rho_{in} = 0$ the CQC method is reduced to SRSS, i.e. well separated frequencies.

The underlying theory behind SRSS and CQC is not presented here but the it can be derived from random vibration theory. If a series of earthquakes is represented by a mean spectrum, CQC and SRSS provides an estimation of the peak response that is close to the mean of the peak responses due to individual earthquakes.

2.3.9 Multi directional response summation

The theory so far has only dealt with earthquake excitation in one given direction. The participation factor Γ_n was derived from a unit ground displacement and any given response entity r_{no} can only be interpreted as the response due to a ground motion excited in the same direction as the direction from which the participation factor was derived.

Since the direction of an earthquake normally is unknown it is fair to say that a building should be able to resist an earthquake from any given direction. It is possible to retrieve the worst response without calculating the participation factors $\Gamma_{n,\theta}$ for every direction θ-degrees about the main axis. Assuming the worst response r_0 is obtained by spectral input along an axis ξ which is aligned θ degrees about the x-axis as shown in Figure 12.

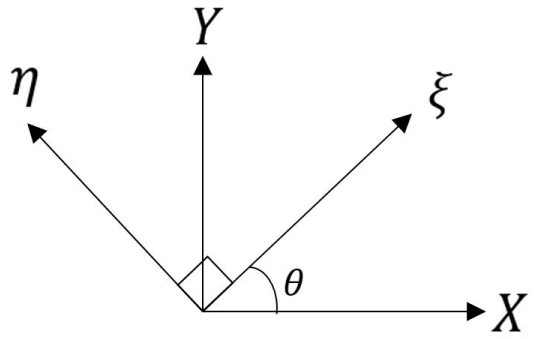

Figure 12: Possible directions of excitation.

The spectral input S_ξ would yield the same response r_0^2 as summing the square roots of the response r_0 due to spectral input along the main axis x and y:

$$r_0(S_\xi)^2 = r_0(S_x)^2 + r_0(S_y)^2 \tag{59}$$

regardless of the angle θ. Consequently, the largest response is found with use of SRSS from orthogonal excitations:

$$r_0(\max) = \sqrt{r_0(S_x)^2 + r_0(S_y)^2} \tag{60}$$

This means that two separate earthquake analysis can be made in two orthogonal directions x and y with two participation factors $\Gamma_{n,x}$ and $\Gamma_{n,y}$ for each mode if a three dimensional behavior of the structure is expected.

3 Seismic design in Eurocode

3.1 Importance factor

In Ec8 the way to differentiate constructions from each other, with regard to reliabilities, is with the use of an importance factor, γ_l [4]. The importance factor is determined in relation to four different importance classes. These classes are determined from the consequence of collapse for human lives, the importance for public safety and civil protection immediately after an earthquake and the social and economical consequence after a collapse. In Table 1 the classes and recommended corresponding factors are presented.

Table 1: Definition of Importance classes and correlated recommended Importance factors.

Importance Class	Building type	Importance factor, γ_I (recommended value)
I	Buildings of minor importance e.g. agricultural buildings, etc.	0.8
II	Ordinary buildings not belonging in the other categories	1.0
III	Buildings whose seismic resistance is of importance in view of the consequences associated with a collapse, e.g. schools, assembly halls, cultural institutions etc.	1.2
IV	Buildings whose integrity during earthquakes is of vital importance for civil protection, e.g. hospitals, fire stations, power plants, etc.	1.4

The factor is used by directly applying it to the hazard value, in this case PGA, a_{gR}:

$$a_g = \gamma_I \cdot a_{gR} \tag{61}$$

The factors presented in Table 1 are, as previously stated, recommended values. These values are NDP's which are determined along with each countries policies for seismic safety and the characteristics of the countries seismic hazard. When using the factor an approximation of a higher or lower probability of exceedance, in T_{LR} years, is achieved expressed in the reference seismic actions probability of exceedance in T_L years. The different characteristics between various levels of seismicity is represented by the seismicity exponent k. The seismicity exponent, k, is recommended to be set to 3. This represents a region of high seismicity e.g. Italy [10]. Lower values of k corresponds to areas with lower seismicity. The relation between the importance factor, different return periods and

how it varies with the seismicity exponent is presented in Figure 13, which is a plot of the relation in equation 62.

$$\gamma_I \sim (T_{LR}/T_L)^{-1/k} \tag{62}$$

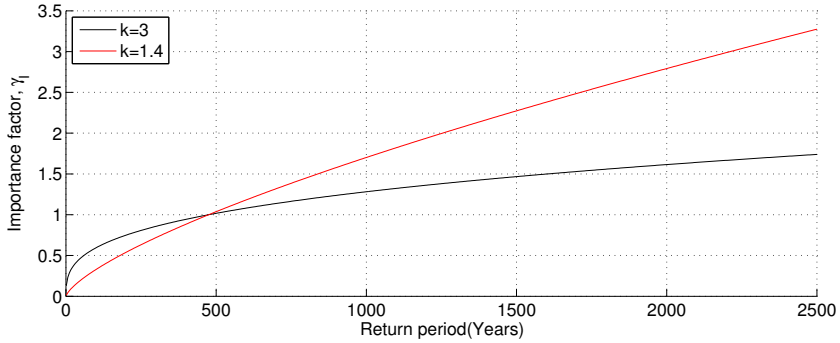

Figure 13: Relation between Importance factor and return periods with different k-values.

The k-value originates in seismic hazard curves [11]. The hazard curves are plotted in a double-logarithmic space. When retrieving the k-value one makes the assumption that the return periods of interest, in connection to structural engineering, is approximately linear within the log-log space that the hazard curve is plotted in, see Figure 14. A k-value approximation of Lund, Sweden is presented in Figure 14. The approximation is made within a range of return periods of 75 to 5000 years.

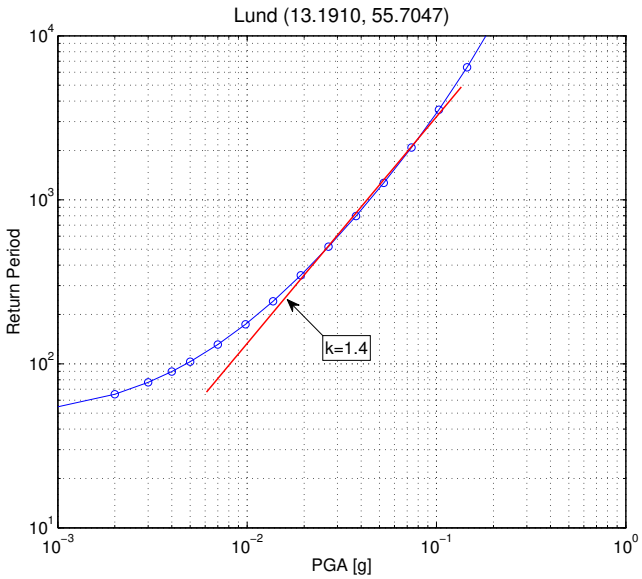

Figure 14: Linear approximation of hazard curve, describing the hazard in Lund.

The implicit return periods correlated to the recommended importance factors for $k = 3.0$ is presented in Table 2. In Table 3 the importance factors have been scaled in order to match the same implicit return periods for $k = 1.4$ as for $k = 3.0$. It can be observed that there is a significant difference of the importance factor in importance class IV for $k = 1.4$ to reach the same implicit return period as for $k = 3.0$.

Table 2: Recommended importance factors and correlated implicit return periods ($k = 3.0$).

Importance class	Importance factor, γ_I	Implicit return period(years)
I	0.8	243
II	1.0	475
III	1.2	821
IV	1.4	1303

Table 3: Scaled importance factors and correlated implicit return periods for $k = 1.4$.

Importance class	Importance factor, γ_I	Implicit return period(years)
I	0.6	243
II	1.0	475
III	1.5	821
IV	2.1	1303

It should be emphasized that the method to approximate the k-value from a hazard spectra is not explicitly stated in Eurocode 8. The method is described in the documentation related to the SHARE project, more specifically in D2.2-Report on seismic hazard definitions needed for structural design applications [12]. To put the scaled importance factor in perspective it could be compared to the factors Norway, who recently adopted Ec8, are currently using. According to Norway's national annex the importance factor correlating to importance class IV is set to 2.0 [13].

3.2 Elastic Design Spectrum

Eurocode gives the user an option of analyzing structures with a scaled design spectrum. By introducing a behavior factor q the spectrum is scaled according to a type of building, e.g. building materials, stabilizing system etc. The behavior factor takes the structures ability to dissipate energy into account and therefore a simpler analysis can be performed without any further attention to inelastic behavior [14]. The elastic design spectrum is assembled with equations 63-66[4].

$$0 \leq T \leq T_B : S_d(T) = a_g \cdot S \cdot \left[\frac{2}{3} + \frac{T}{T_B} \cdot \left(\frac{2.5}{q} - \frac{2}{3}\right)\right] \tag{63}$$

$$T_B \leq T \leq T_c : S_d(T) = a_g \cdot S \cdot \frac{2.5}{q} \tag{64}$$

$$T_C \leq T \leq D_c : S_d(T) = \begin{cases} a_g \cdot S \cdot \frac{2.5}{q} \cdot \left[\frac{T_C}{T}\right] \\ \geq \beta \cdot a_g \end{cases} \tag{65}$$

$$T_D \leq T : S_d(T) = \begin{cases} a_g \cdot S \cdot \frac{2.5}{q} \cdot \left[\frac{T_C T_D}{T^2}\right] \\ \geq \beta \cdot a_g \end{cases} \tag{66}$$

Where

$S_d(T)$	is the elastic design spectrum;
T	is the vibration period of a linear single-degree-of-freedom system;
a_g	is the design ground acceleration on type A ground;
T_B	is the lower limit of the period of constant spectral acceleration branch;
T_C	is the upper limit of the period of constant spectral acceleration branch;
T_D	is the value defining the beginning of the constant displacement response range of the spectrum;
S	is the soil factor;
q	is the behavior factor;
β	is the lower bound factor for the horizontal design spectrum (recommended value 0.2).

The design ground acceleration, a_g, is calculated with equation 61, using the importance factor and the reference peak ground acceleration, a_{gR}, on ground type A. Ground type A means rock or rock-like formations with less than 5 meters of weaker material at the surface with a shear wave velocity, $v_{s,30}$, of >800 m/s. The shear wave velocity is calculated as an average velocity of all layers in the top 30 meters of the ground. In Table 4 all ground types are defined. In order to account for different ground types the soil factor, S, is used to scale the design spectrum[14].

Table 4: Description of ground types[4] and correlated parameters.

Ground type	Description of stratigraphic profile	Parameters		
		$v_{s,30}$ (m/s)	N_{SPT} $(blows/30cm)$	c_u (kPa)
A	Rock or other rock-like geological formation, including at most 5 m of weaker material at the surface.	>800	-	-
B	Deposits of very dense sand, gravel, or very stiff clay, at least several tens of meters in thickness, characterized by a gradual increase of mechanical properties with depth.	360 – 800	>50	>250
C	Deep deposits of dense or medium dense sand, gravel or stiff clay with thickness from several tens to many hundreds of meters.	180 – 360	15 - 50	70 - 250
D	Deposits of loose-to-medium cohesionless soil (with or without some soft cohesive layers), or of predominantly soft-to-firm cohesive soil.	<180	<15	<70
E	A soil profile consisting of a surface alluvium layer with v_s values of type C or D and thickness varying between about 5 m and 20 m, underlain by stiffer material with $v_s > 800$ m/s.			
S1	Deposits consisting, or containing a layer at least 10 m thick, of soft clays/silts with a high plasticity index (PI >40) and high water content	<100 (indicative)	-	10 - 20
S2	Deposits of liquefiable soils, of sensitive clays, or any other soil profile not included in types A – E or S_1			

Dependent on a regions seismicity two different types of spectra are recommended. These spectra are based on earthquakes magnitude that contributes most to an areas seismicity. For areas of high seismicity that satisfies the condition, $M_s > 5.5$, a Type 1 spectrum is can be used. For areas of lower seismicity, $M_s \leq 5.5$, a Type 2 spectrum can be used.

These spectra are defined with the intention of not overestimate the spectral ordinates for areas that are not subjected to high magnitude earthquakes. In Table 5 the recommend values for a Type 2 spectrum are presented. Depending on what ground type that is chosen, values describing the soil factor and the corner periods are determined.

Table 5: Values of parameters describing Type 2 spectrum(recommended values)[14].

Ground type	S	$T_B(s)$	$T_C(s)$	$T_D(s)$
A	1.0	0.05	0.25	1.2
B	1.35	0.05	0.25	1.2
C	1.5	0.10	0.25	1.2
D	1.8	0.10	0.30	1.2
E	1.6	0.05	0.25	1.2

The design spectrum is calibrated for a vicious damping (ξ) of 5%. Other values of damping can be used by the means of adjusting the factor q in accordance to specific building materials. When concrete is used as the primary building material the q factor, for low seismicity cases, is allowed to be chosen between 1-1.5. This also gives the opportunity of designing the concrete elements according to Eurocode 2[4].

3.3 Integration of SHARE outputs with Eurocode 8

If the seismic hazard in Lund predicted by SHARE is plotted together with the design spectrum given in Eurocode 8 with recommended parameters it becomes obvious that the design spectrum grossly overestimate the seismic hazard in Lund as seen in Figure 15 . The design spectrum is calculated for Ground type A and a behavior factor $q = 1$. The reference ground acceleration $a_g = 0.02$g is the peak ground acceleration.

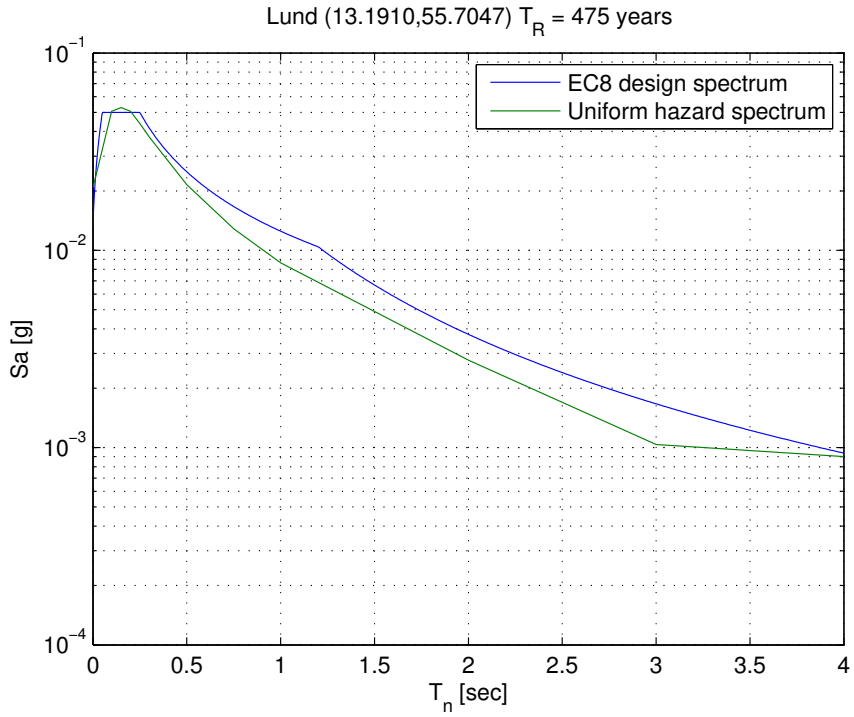

Figure 15: Comparison of design spectrum and uniform hazard spectrum in Lund for return period of 475 years.

It can be seen that the spectral acceleration is higher for almost every spectral period T_n and the constant acceleration branch seems wider than necessary. Arguably, the UHS could be used directly in a seismic analysis, instead of a design spectrum, since it predicts the actual hazard at site. However, the design spectrum, which is an idealized UHS, have e.g. a branch of constant spectral acceleration which inhibits large response differences for small model deviations.

SHARE provides a method [11] to better estimate the parameters in Table 5 in order to fit the design spectrum to the UHS for a specific site. Their results for Lund is provided in Table 6.

Table 6: Eurocode 8 controlling parameters (T_B, T_C and T_D) optimized to fit the SHARE uniform hazard spectrum in Lund.

$T_B(s)$	$T_C(s)$	$T_D(s)$
0.1	0.2	1.0

The design spectrum was calculated according to Eurocode 8 but with the spectral period limits according to Table 6. Note that the soil factor $S = 1$ is still assumed, i.e. ground type A, according to Table 5. This assumption is made since the hazard calculated in SHARE is only provided for a shear wave velocity $v_{s,30} = 800m/s$ which makes a fair comparison to Ground type A, see Table 4. Ground types other than A is beyond the

scope of this project but it should be noted that other ground types can magnify the seismic action significantly. The design spectrum is shown in Figure 16.

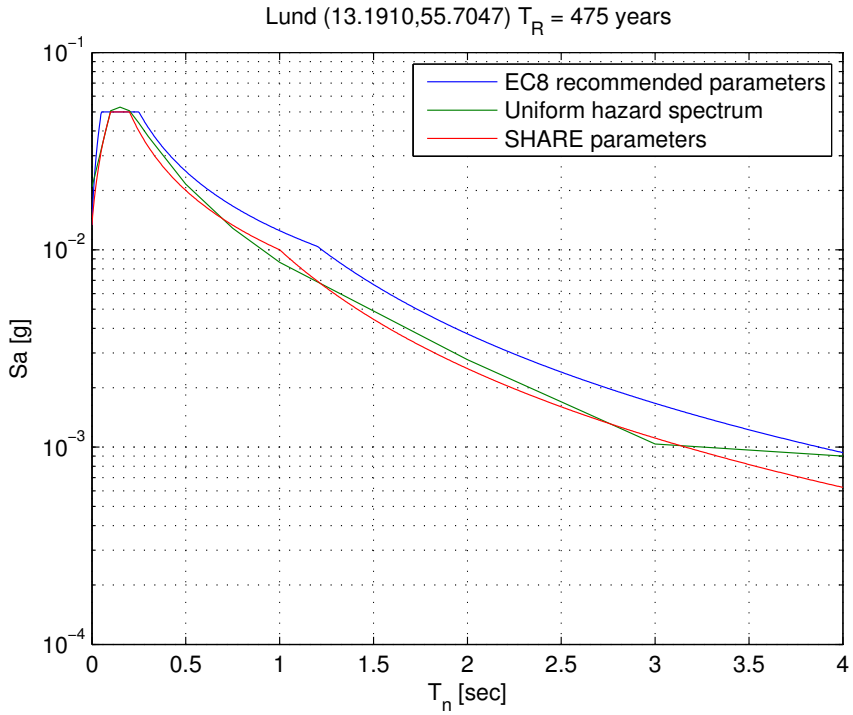

Figure 16: Design spectrum with SHARE parameters in Lund for a return period of 475 years.

The SHARE parameters provide a much better fit to the UHS. It is far less conservative than the recommended EC8 spectra with lower values and a more narrow constant acceleration branch.

The way to differentiate reliabilities with use of an importance factor γ_1 have a little merit when the seismic hazard already is calculated for a large range of return periods. The importance factor essentially scales a reference ground acceleration to another ground acceleration with a different return period. Since SHARE provides PGA for return periods up to 5000 years the importance factor is redundant and the PGA for a return period of choice can be selected. It was however concluded that the recommended importance factor $\gamma_1 = 1.4$ implicitly means a return period of $\sim$ 1300 years. However, the return period remains a matter of choice for national authorities to decide and it is impossible to predict how Swedish authorities would approach this issue if Eurocode 8 ever would be implemented in Sweden. In this paper, it is assumed a return period T_R of 1300 years is a reasonable choice for for building in importance class IV.

The reference ground acceleration for $T_R = 1300$ years are $a_g = 0.054$g. The value was interpolated from the hazard curve in Figure 17.

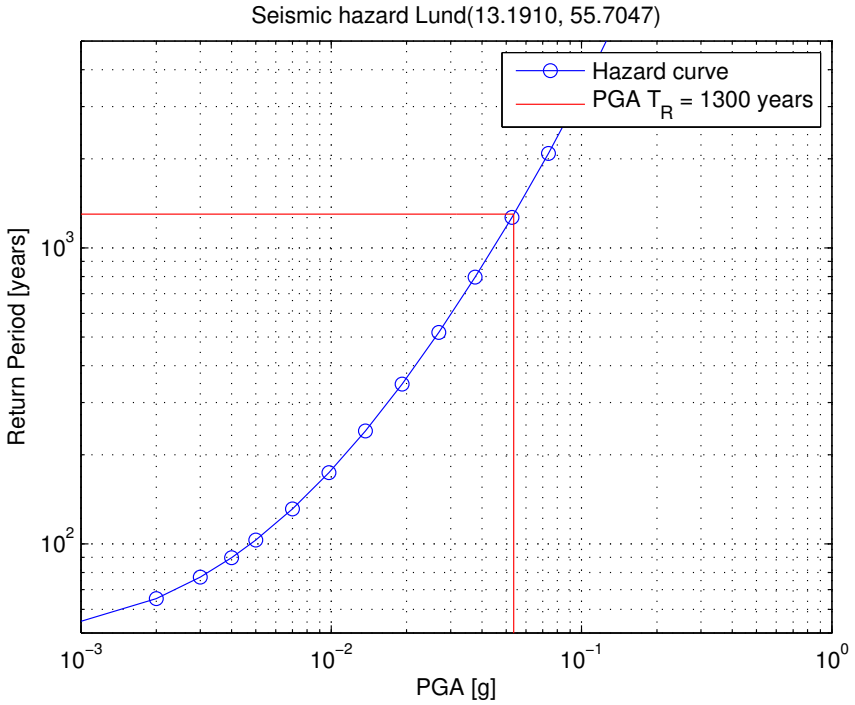

Figure 17: Hazard curve Lund, $T_R = 1300$ and $a_g = 0.054$g in red.

The design spectrum for $T_R = 1300$ years was assembled with parameters according to SHARE, soil factor $S = 1$ and reference ground acceleration $a_g = 0.054$g. The 1300-year spectra is shown in Figure 18 together with the 475-year spectra.

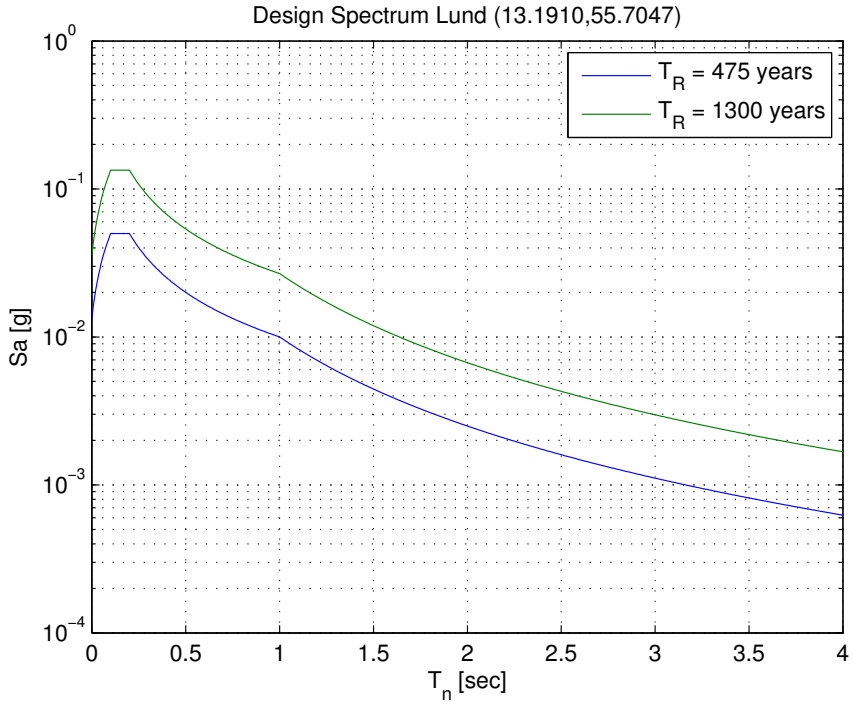

Figure 18: Design spectrum used in this project.

4 Method

The way to evaluate the seismic action were made using three different analyzes. The first one, presented in section 5, was a parametric study of idealized structures where a large number of different buildings were modeled as 2D-beams subjected to a seismic load as a modal response spectrum analysis. The analyses were made using the 475- and 1300-year spectra presented in Figure 18 and the results were presented together with a static analysis of the wind load. The purpose was to identify general characteristics of buildings that can be considered to be critical to earthquake loads. Only the base shear force was evaluated since it is a good indicator of how large the response is in general. A more detailed description of the analysis is presented in Section 5.

The second analysis was a parametric study of a 3D-model in the FE-software Abaqus. The base shear response were calculated with a varying number of floors (4 to 7 floors). The purpose was to investigate how well the beam models can predict the response in buildings that deviates from ideal properties. Equivalent beam properties were estimated from the 3D-model and the response were calculated with these properties using the beam model. A more detailed description of the analysis is presented in Section 6.

The third analysis, presented in section 7, was a case study based on the worst case scenario from the latter analysis. The FE-model from the second analysis was used with a fixed number of floors. The study was investigating section forces and moments from static wind loads and dynamic earthquake loads. Both a 475- and a 1300-year spectra was used. The purpose of the case study was to evaluate the use of base shear as a measure of comparison in the previous analyzes. The study also provides a description of possible differences between the static wind load and dynamic earthquake loads.

5 Parametric study of idealized structures

Since wind usually is the designing horizontal load in Sweden it is of interest to find a structural system that is able to produce an earthquake response that is relatively high compared to the wind load. In this section the base shear force in idealized structures are compared for both load types by parameterizing several structural properties. The purpose is to identify the general characteristics of buildings that can be considered to be critical to earthquake loads.

5.1 Method of analysis

5.1.1 Model description

A rectangular building with N stories is subjected to analysis. Each story is h meters high and the sides of the building are d and w meters each. The floors are assumed to be 0.3 m thick solid concrete slabs with a density of 2400 kg/m^2. The vertical system is comprised of an arbitrary amount of continuous elements. The mass of the building is concentrated to the slabs.

The building is modeled as a vertical 2D cantilever beam with one elastic Bernoulli beam-element between each floor. Hence, the degrees of freedom are located at the center of each floor slab.

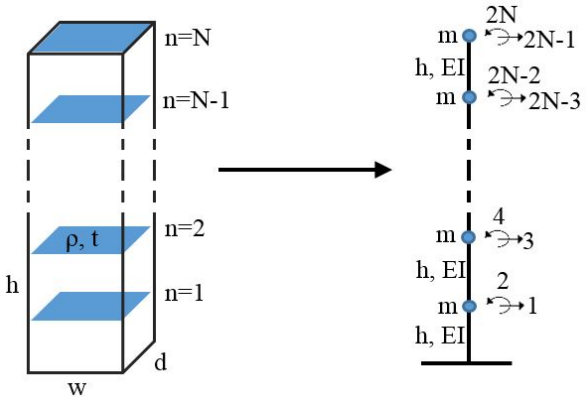

Figure 19: Illustration of cantilever beam model.

The element stiffness matrix is given by:

$$\boldsymbol{K_E} = \begin{bmatrix} 12EI/h^3 & 6EI/h^2 & -12EI/h^3 & 6EI/h^2 \\ 6EI/h^2 & 4EI/h & -6EI/h^2 & 2EI/h \\ -12EI/h^3 & -6EI/h^2 & 12EI/h^3 & -6EI/h^2 \\ 6EI/h^2 & 2EI/h & -6EI/h^2 & 4EI/h \end{bmatrix} \tag{67}$$

where EI is the equivalent stiffness of some amount of vertical elements contributing to the horizontal stability. In this analysis EI is a parameter rather than explicitly obtained from material properties, element shape and number of elements. Obviously, the parameter EI has to be chosen within an appropriate range of values which are reasonable for the model. Appropriate values of EI is highly dependent on stabilizing system (columns, shear walls, etc.) but this topic is discussed later.

The element mass matrix for a Bernoulli beam-element is given by:

$$\boldsymbol{M_E} = \frac{\hat{m}h}{420}\begin{bmatrix} 156 & 22h & 54 & -13h \\ 22h & 4h^2 & 13h & -3h^2 \\ 54 & 13h & 156 & -22h \\ -13h & -3h^2 & -22h & 4h^2 \end{bmatrix} \tag{68}$$

where $\hat{m}$ is mass per unit length of the beam. The element matrices are assembled into a global matrix $\boldsymbol{M}_{beam}$. The floor masses m_i are directly assembled into the global matrix, as lumped masses in the diagonal for every 1 to N matrix element corresponding to a global translational degree of freedom.

$$\boldsymbol{M}_{floor} = \begin{bmatrix} m_1 & 0 & \cdots & \cdots & \cdots & \cdots & 0 \\ 0 & 0 & \cdots & \cdots & \cdots & \cdots & 0 \\ 0 & 0 & m_2 & \cdots & \cdots & \cdots & 0 \\ \vdots & \vdots & \vdots & \ddots & \vdots & \vdots & \vdots \\ 0 & \cdots & 0 & 0 & m_{N-1} & 0 & 0 \\ 0 & \cdots & \cdots & 0 & 0 & 0 & 0 \\ 0 & \cdots & \cdots & \cdots & \cdots & 0 & m_N \end{bmatrix} \tag{69}$$

The global mass matrix becomes:

$$\boldsymbol{M} = \boldsymbol{M}_{beam} + \boldsymbol{M}_{floor} \tag{70}$$

In reality, the slabs contribute to rotational stiffness at floor level. The stiffness contribution from the slabs is however difficult to estimate and to include as a parameter since the stiffness is dependent on, aside from the slab's own properties, the spatial distribution of the vertical elements of which the slabs are connected to. For instance the slab in Figure 20 contributes to more rotational stiffness about the x-axis than the y-axis since the columns are closer spaced in the y-direction.

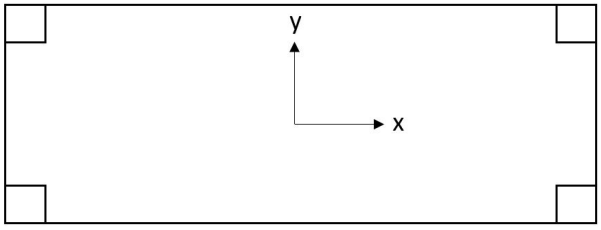

Figure 20: Rectangular slab on four columns.

To clarify the fact that the frame is stiffer about the x-axis, it can be seen in Figure 21 that the rotational stiffness at the corner (k_{22}) of the frame is dependent on the length of the span between columns.

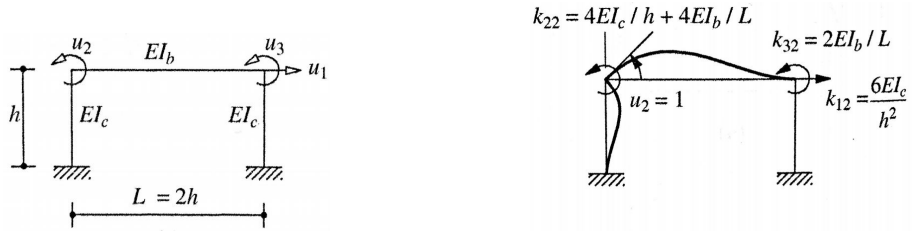

(a) (b)

Figure 21: Explanation of slab stiffness contribution.

Instead, the structure is analyzed from two extreme cases with regards to the stiffness ratio ρ between the slabs and the vertical elements:

- Case 1: $\rho = 0$
- Case 2: $\rho = \infty$

For Case 1 it is implied that the stiffness contribution from the slabs is negligible. This is based on the assumption that the vertical elements are exceptionally stiff compared to the slabs. For such assumption to be legitimate, the building is likely to be stabilized with stiff elements like elevator shafts and/or shear walls with high moment of inertia. This building is assumed to behave like a cantilever beam when subjected to lateral forces.

On the contrary, in Case 2 it is implied that the structure is stabilized with relatively slender vertical elements, for instance a system of columns. When subjected to lateral forces, the slabs shear the columns and cause horizontal translations without rotations at floor level. Figure 22 demonstrates the principal difference between Case 1 and 2 for a multi story frame.

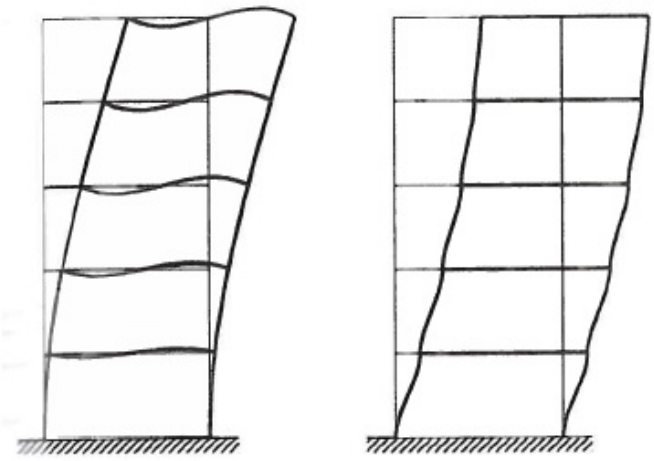

Figure 22: Multi story frame building, case 1 (left) and case 2 (right).

From here on Case 1 is referred to as **cantilever building** and Case 2 is referred to as **shear building**. It's worth pointing out that both buildings are modeled as one cantilever beam with one Bernoulli beam element between each floor. However, the rotational degrees of freedom are condensated using boundary conditions in the shear building.

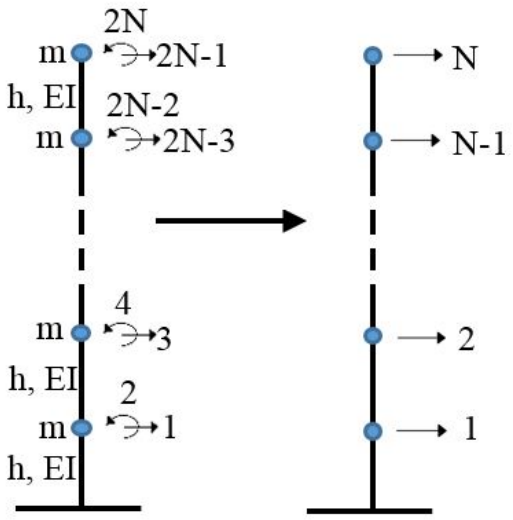

Figure 23: Cantilever building (left), Shear building (right).

Essentially the element stiffness matrix in (67) is reduced to a 2 by 2 matrix for the shear building:

$$\boldsymbol{K_E} = \begin{bmatrix} 12EI/h^3 & -12EI/h^3 \\ -12EI/h^3 & 12EI/h^3 \end{bmatrix} \tag{71}$$

The mass in the vertical elements $\hat{m}$ is assumed to be zero for the shear building. The cantilever building has however a distributed mass $\hat{m} = 7200$ kg/m which is equivalent to a 10 m by 0.3 m concrete wall. The results are not sensitive to this parameter since the floors are much heavier and this is why a constant value of $\hat{m}$ was assumed. The global mass matrix for the shear building becomes:

$$\boldsymbol{M} = \begin{bmatrix} m_1 & 0 & \cdots & \cdots & 0 \\ 0 & m_2 & \cdots & \cdots & 0 \\ \vdots & \vdots & \ddots & \vdots & \vdots \\ 0 & \cdots & 0 & m_{N-1} & 0 \\ 0 & \cdots & \cdots & 0 & m_N \end{bmatrix} \tag{72}$$

Since $\boldsymbol{M}_{beam} = \boldsymbol{0}$ and all degrees of freedom are horizontal translations.

5.1.2 Parameters

The building is assumed to have a constant floor height $h = 3.5$ m and slab thickness 0.3 m. The response in the building is investigated for different stiffness EI, building depth d, building width w and number of floors.

Table 7: Parameters and their range that are to be investigated.

Parameter	Symbol	Variation Range	
		From	To
Number of floors	N	1	8
Depth	d	10 m	40 m
Width	w	10 m	40 m
Stiffness shear building	EI	0.1 GNm^2	5 GNm^2
Stiffness cantilever building	EI	100 GNm^2	2000 GNm^2

The investigated range of bending stiffness EI in Table 7 was derived from a range of concrete elements with different dimensions. For the shear building the stiffness was calculated for circular concrete columns with an elastic modulus $E = 35$ GPa and moment of inertia I given by:

$$I = n \cdot \frac{\pi r^4}{4} \tag{73}$$

where r is the radius and n is the number of columns at each floor level. Similarly, the stiffness range for the cantilever building was derived from a range of 0.3 m thick concrete walls with a moment of inertia given by:

$$I = n \cdot \frac{0.3 \cdot y^3}{12} \tag{74}$$

where y is the wall depth and n is the number of walls at each floor level. The upper and lower bound for EI for both models was somewhat arbitrarily chosen to cover a reasonable range of stiffness. The chosen values in Table 7 are shown together with values of EI calculated from Equation 73 and 74 in Figure 24.

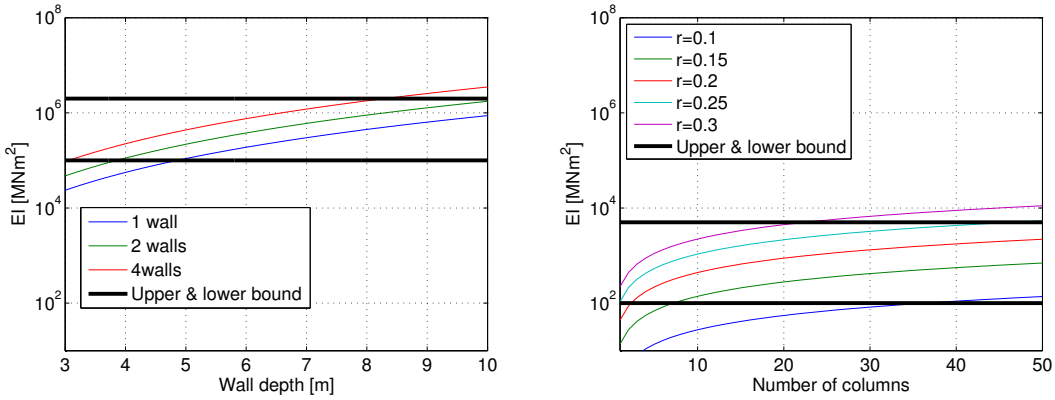

(a) (b)

Figure 24: Upper and lower bound for investigated parameter EI. Cantilever building (a) and shear building (b).

A set of five discrete values of EI within the bounds were analyzed for eight buildings with one to eight stories N and a constant depth and width $d = w = 20$ m. The method of analysis was *Modal response spectrum analysis* and it was performed for both the cantilever and shear building. In total the earthquake response for 80 different buildings were calculated.

The base response in a building with a surface area $S = d \cdot w$ can be scaled linearly for a similar building with a surface area $S' = d' \cdot w'$ (for same stories N). If both buildings have the same amount of stabilizing elements per square meter, i.e. constant ratio between stiffness and mass k/m, the eigen frequencies remains unchanged:

$$\omega_n = \sqrt{\frac{k}{m}} = \sqrt{\frac{k'}{m'}} \tag{75}$$

Since the eigen frequencies are the same for both buildings the modal response ratio $V_{bn}(A')/V_{bn}(A)$ is equal to the mass ratio since the modal acceleration $A_n = A'_n$:

$$\frac{V_{bn}(A'_n, M'_n)}{V_{bn}(A_n, M_n)} = \frac{M'_n A'_n}{M A_n} = \frac{M'_n}{M_n} \tag{76}$$

where M_n is the effective modal mass. The modal response can thus be scaled accordingly:

$$V'_{bn} = \frac{M'_n}{M_n} V_{bn} \tag{77}$$

Since the modal response can be scaled, the total response can also be scaled similarly:

$$V_b' = \frac{M'}{M} V_b \tag{78}$$

where M is the total mass of the building. Since the mass is proportional to the surface area, different values of d and w can be chosen to scale the results for smaller and larger buildings:

$$V_b' = \frac{d' \cdot w'}{d \cdot w} V_b \tag{79}$$

As a consequence the base shear is increased with a factor of 4 when the side lengths are doubled. This can be compared to the response from the wind load, where the base shear is only increased with a factor of 2. Furthermore, a building that is only elongated with a factor 2 in one direction have an unchanged wind response in the same direction. The earthquake response however is doubled.

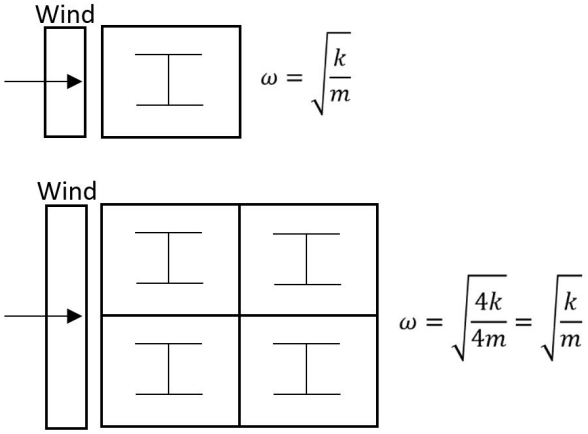

Figure 25: Building comprised of four modules. This configuration yields wind response x2 and seismic response x4 since the eigen frequencies remains unchanged but the mass is quadrupled.

With the size effect in mind, it is self evident that it is possible to find a building that is able to produce an earthquake response that envelopes the wind response. Therefore, the parameters d and w in Table 7 are only investigated in terms of *largest theoretical base shear* in order to demonstrate the size effect. The largest theoretical base shear can be calculated by assuming that the total mass M is excited with a frequency corresponding to the largest spectral acceleration Sa_{max}.

$$V_{b,max} = M \cdot Sa_{max} \tag{80}$$

It should be clarified that the *size effect* as previously defined, does not change the seismic response in each member, as both the total seismic response and the number of stabilizing members are proportional to the size given all assumptions previously presented in this section. The wind response in each member would however decrease since the total wind response is only proportional to one side of the building.

5.1.3 Seismic load

The type 2 elastic design spectrum according to Eurocode 8 and SHARE parameters was chosen in this analysis, see Equations 63 to 66. The analysis was made for and importance class II and IV, i.e. the reference ground acceleration corresponds to a return period of 475 years and 1300 years respectively.

See Figure 18 in Section 3.3 for complete spectra.

The modal response summation method used was SRSS.

5.1.4 Wind load

The seismic response in this parametric study are presented together with the same response for wind load. The wind load is calculated according to SS-EN-1991-1-4 [6] with the following parameters:

- Reference wind speed $v_b = 26$ m/s
- Terrain type III

The wind is assumed to act with a constant pressure on the facade corresponding to the pressure at the highest point of the building.

The comparison of wind and seismic response was made in the context of a design situation. In general, the following condition have to be fulfilled in the ultimate limit state:

$$\frac{R_k}{\gamma_M} \geq E_d \tag{81}$$

where R_k is the characteristic value of the capacity and E_d is the designing load effect. The partial coefficient γ_M takes model uncertainties into account and for a "normal" design situation, like wind action, γ_M takes the value 1.5 for concrete materials. However, Eurocode treats seismic action as an *exceptional design situation* where γ_M takes the value 1.2, i.e. uncertainties are accepted to a larger degree.

In order to compare the wind action to the seismic action, the wind pressure is modified, $Q_{d,mod}$ in Equation 82, with respect to the uncertainty acceptance of the capacity, using a factor of the ratio between γ_M for both design situations.

$$Q_{d,mod} = \frac{1.5}{1.2} \cdot Q_d \tag{82}$$

Q_d is the designing wind pressure and it is design in the the ultimate limit state, thus the characteristic wind pressure is multiplied with 1.5 according to Equation 83.

$$Q_d = 1.5 \cdot Q_k \tag{83}$$

By combining Equation 82 and 83, the factor that is multiplied with the wind load becomes:

$$Q_{d,mod} = \frac{1.5}{1.2} \cdot 1.5 \cdot Q_k \tag{84}$$

As a note, the seismic load is an accidental load case where the load combination factor is equal to 1.0:

$$A_d = 1.0 \cdot A \tag{85}$$

5.2 Results

5.2.1 Analysis of modes and effective mass

Before examining the response it is interesting to see how the effective mass is distributed between the modes. For a 8-story building the effective mass is presented in Figure 26 as a percentage of the total mass.

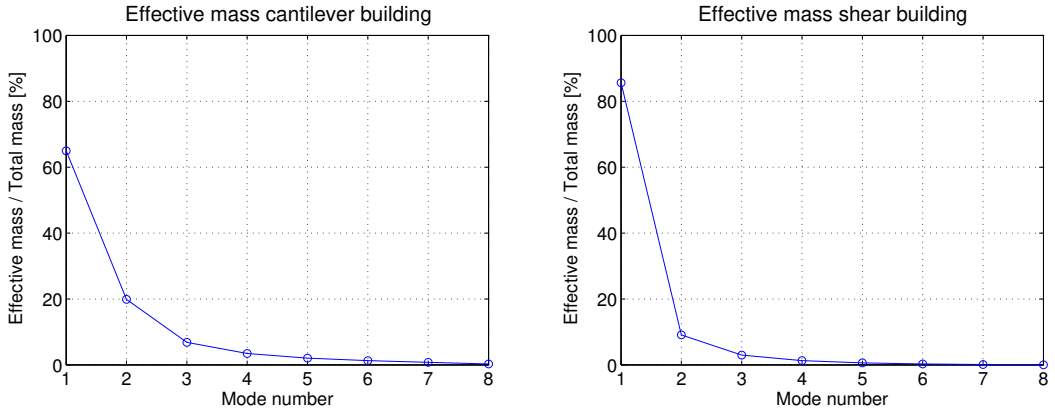

(a) (b)

Figure 26: Effective mass content in each mode for the cantilever building (a) and the shear building (b).

The cantilever building has $\sim 65\%$ effective mass in the first mode while the shear building has $\sim 85\%$. This goes to show why it was important to separate these models. The stiffness cannot be arbitrary chosen without considering the stiffness ratio between the slabs and vertical members since more effective mass will be distributed from the first mode to the others the more rigid the vertical members become compared to the slabs. The implications are that the shear building is very dependent on the spectral ordinate of the first mode. If this is located in the constant acceleration branch of the spectra (between 0.1 and 0.2 seconds) the base shear is expected to almost reach the largest theoretical base shear, i.e:

$$V_b(0.1s < T_1 < 0.2s) \approx Sa(\max) \cdot M_{tot} \tag{86}$$

The cantilever building however, which is only $\sim 65\%$ dependent on the spectral ordinate of the first mode, will also have a significant contribution from the second mode $\sim 20\%$.

The differences in the distribution of the effective mass can be found in the different mode shapes, see Figure 27.

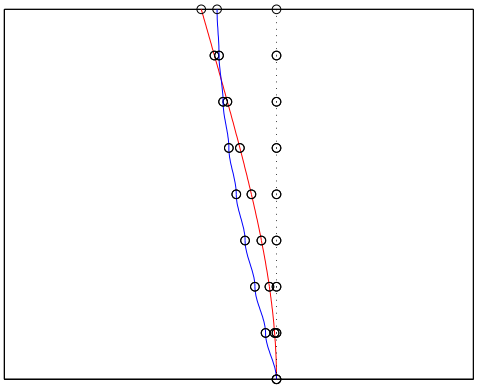

Figure 27: Comparison of first mode shape. Blue: Shear building, Red: Cantilever building.

As can be seen the modes are separated in shape and in order to understand why the shear building produce more effective mass in the first mode one has to realize that the effective mass is exactly the same as the static base "shear force" V_{bn}^{st} produced by static distribution of the masses in Figure 27. Both mode vectors in Figure 27 are normalized with respect to the mass, i.e. $M_n = \boldsymbol{\phi}^T \boldsymbol{m} \boldsymbol{\phi} = 1$, which provides an opportunity to visually compare how much static base shear both mode shapes produce. It can be seen that the masses in the shear building have combined been displaced further away relative to the cantilever building thus the static inertia "force" $\boldsymbol{s}_n^T \boldsymbol{\iota}$ is greater.

The same principle works for differences for other modes between both models. A comparison would however be less intuitive since the mode shapes are more complicated to visually compare. The first three mode shapes are presented in Figure 28.

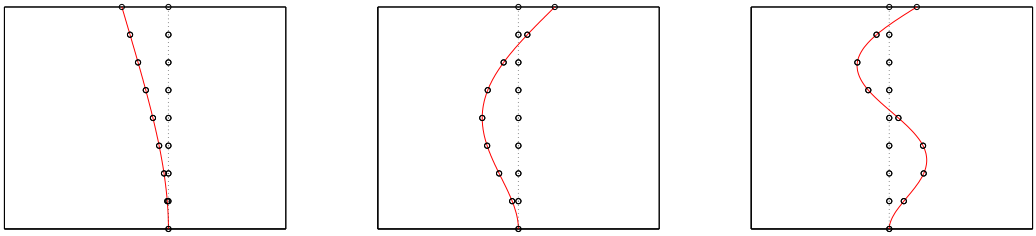

(a) Mode 1 (b) Mode 2 (c) Mode 3

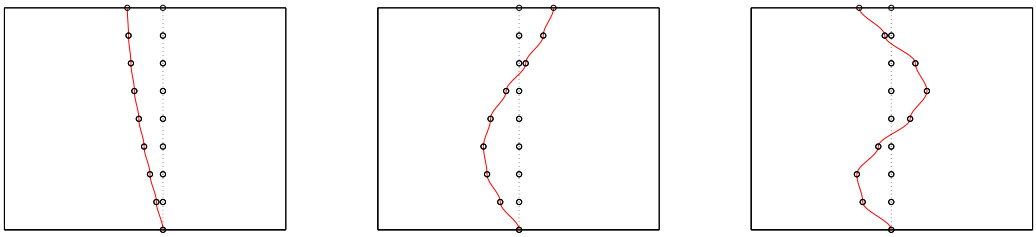

(d) Mode 1 (e) Mode 2 (f) Mode 3

Figure 28: Mode shapes. (a)-(c) Cantilever building. (d)-(f) Shear building.

Higher modes (second and above) must be produced by counteracting inertia forces which is intuitive considering the mode shapes in Figure 28. Consequently, the vector $\boldsymbol{s}_n^T$ contains both positive and negative values hence the total inertia force $\boldsymbol{s}_n^T \boldsymbol{\iota}$ becomes smaller. This explains why the effective mass is significantly lower for higher modes.

5.2.2 Size effect- Largest theoretical base shear

The modal response spectrum analysis were only performed for buildings with a surface area of $20 \cdot 20$ m since it was concluded that a larger or smaller building would only scale the response linearly under the assumption that stiffness/mass ratio remained constant. This size effect is visualized in Figure 29 in terms of largest theoretical base shear. The wind response against the short side were calculated for equivalent buildings and presented in the same plots as dashed lines.

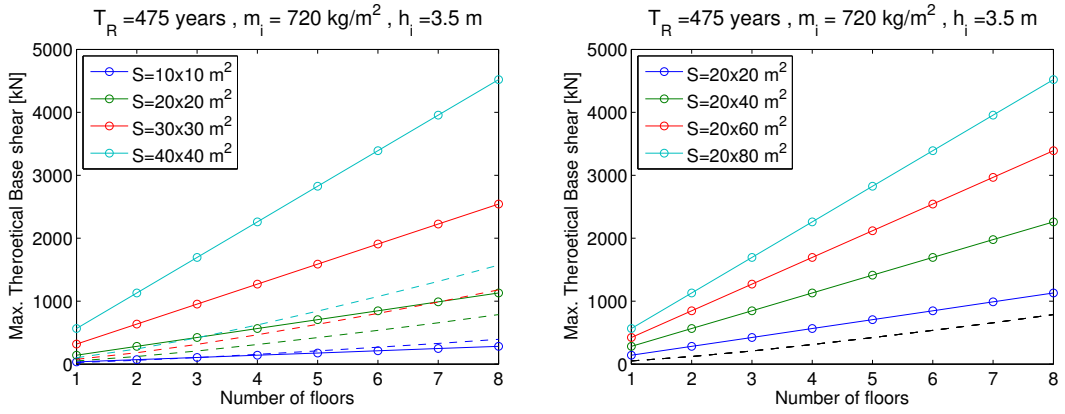

(a) (b)

Figure 29: Largest theoretical base shear. (a) Elongation in both directions, (b) Elongation in one direction.

Figure 29 shows what was mentioned in Section 5.1.2. The seismic responses in buildings with constant stiffness/mass ratio but different surface areas $d \cdot w$ respectively $d' \cdot w'$ are related through

$$V_b' = \frac{d' \cdot w'}{d \cdot w} V_b \tag{87}$$

The wind response is however only proportional to the length of the side of action, i.e.

$$V_{b,wind}' = \frac{w'}{w} V_{b,wind} \tag{88}$$

if the side of action has the length w respectively w'. In Figure 29 (b) the wind is applied at the short side of the building hence constant wind response in the long direction.

Equation 87 and 88 should be kept in mind for the rest of Section 5 since the following results presented in this section are only calculated for 20 m by 20 m buildings. These results were provided just to raise awareness that the seismic response in the forthcoming results would be e.g. four times greater if 40m by 40m buildings (with the same stiffness/mass ratio) were to be analyzed instead.

5.2.3 Shear building

The eigenperiods for the first mode are presented for 40 different shear buildings are presented in Figure 30. These have stiffness EI varying between 100 and 5000 MNm^2 and one to eight stories.

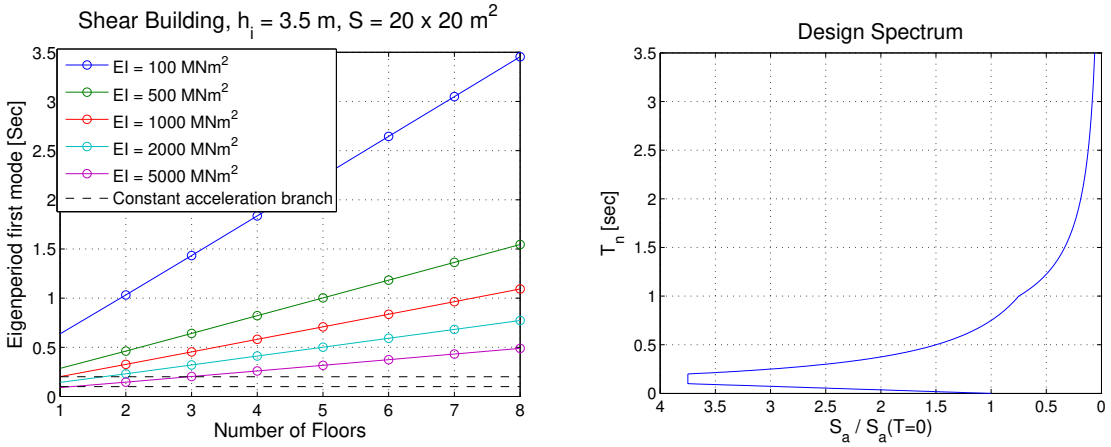

(a) (b)

Figure 30: (a) Eigenperiods first mode for 40 different shear buildings. (b) Relative spectral acceleration.

If the first eigenperiod is within the dashed lines it is located in the constant acceleration branch of the design spectra where the largest spectral accelerations can be found. As was discussed in the previous section, these structures are expected to almost reach the largest theoretical base shear. Most of the shear buildings that were analyzed are slender thus containing high eigenperiods far beyond constant acceleration branch. However, the stiffest building ($EI = 5000$ MNm^2) have, for 1 to 3 floors, the first period within or close to this branch and it can be seen from Figure 31 that these buildings almost tangent the largest theoretical base shear.

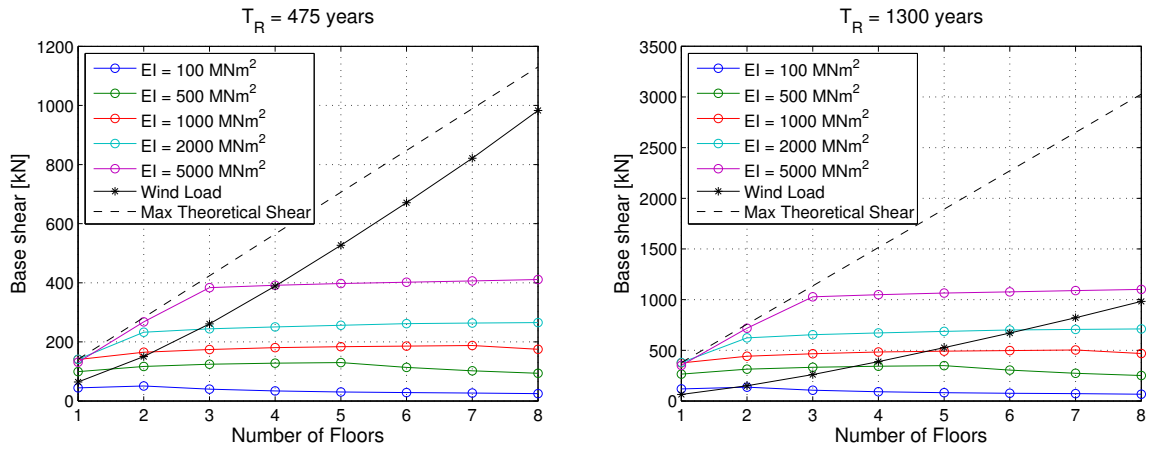

(a) (b)

Figure 31: Shear building response for T_R =475 (a) and T_R =1300 (b).

As shown in Figure 31 (a) the shear building is barely able to produce base shear for the 475-year earthquake that is larger than the wind response. However, some structures with

frequencies close to the constant acceleration branch do. These are however structures with relative low mass (few stories) in relation to the stiffness of the vertical members and there is probably little merit in comparing these results to the wind response. It is likely that other loads, such as accidental loads from impacts, could be the designing load case. Furthermore, this model becomes less accurate with increasing EI since the stiffness is assumed to be infinitely small compared to the stiffness of the slabs. The implications are that the mode shapes, which are key in modal response spectrum analysis, could in practice look more like that of a cantilever beam.

It is safer to say that it is very possible an earthquake with a return period of 1300 years could be the designing load case, referring to Figure 31 (b) as it envelopes the wind response even for more slender and taller buildings. Though, perhaps it is debatable whether these buildings in reality could exist as consequence class IV structures. It could be assumed there is not a single shear wall located in these buildings due to the low stiffness range that was investigated and no emphasis has been made to whether or not these are practical structural solutions or not. The results were provided nonetheless since the buildings in theory could exist.

Due to the low seismic response in general and practical concerns mentioned above the shear building model was not investigated further. In the next section the results from the parametric study of cantilever buildings are presented. These results are more interesting as the seismic response in general is higher and the model has not the same practical issues as the shear building.

5.2.4 Cantilever building

It can be concluded from the analysis of the shear building that these in general were too slender to be able to produce a large seismic response. Although some examples were found that could, the relevance of these results were debatable. However, the cantilever buildings produce in general much more base shear due to seismic loading. The reason is, these buildings are much stiffer thus having first natural frequency closer to the constant acceleration branch for a wider spectrum of buildings, see Figure 32.

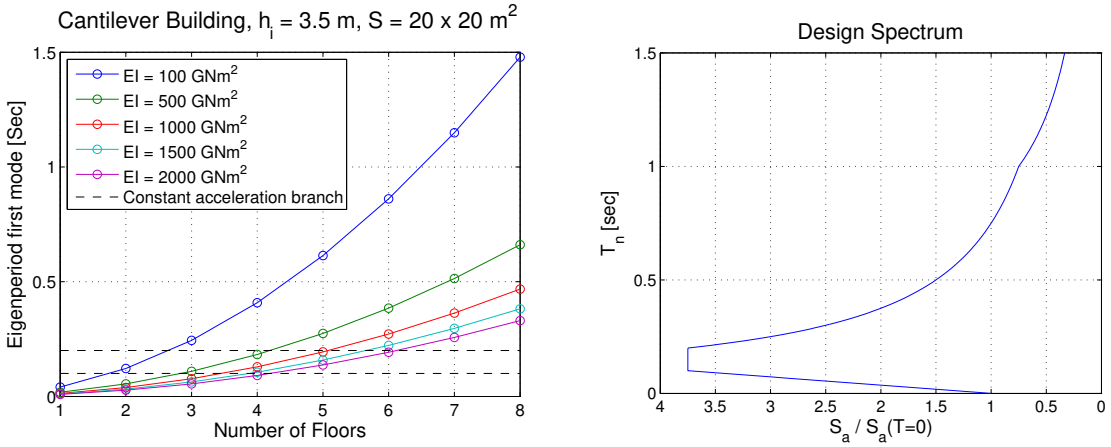

(a) (b)

Figure 32: (a) Eigenperiods first mode for 40 different cantilever buildings. (b) Relative spectral acceleration.

Since the cantilever buildings are, in contrary to the shear buildings, more dependent on higher modes the response is not as linearly associated to the frequency of the first mode but the trend is still the same; cantilever buildings with the first mode in the constant acceleration branch experience the largest base shear in relation to the wind response, comparing Figure 32 and Figure 33.

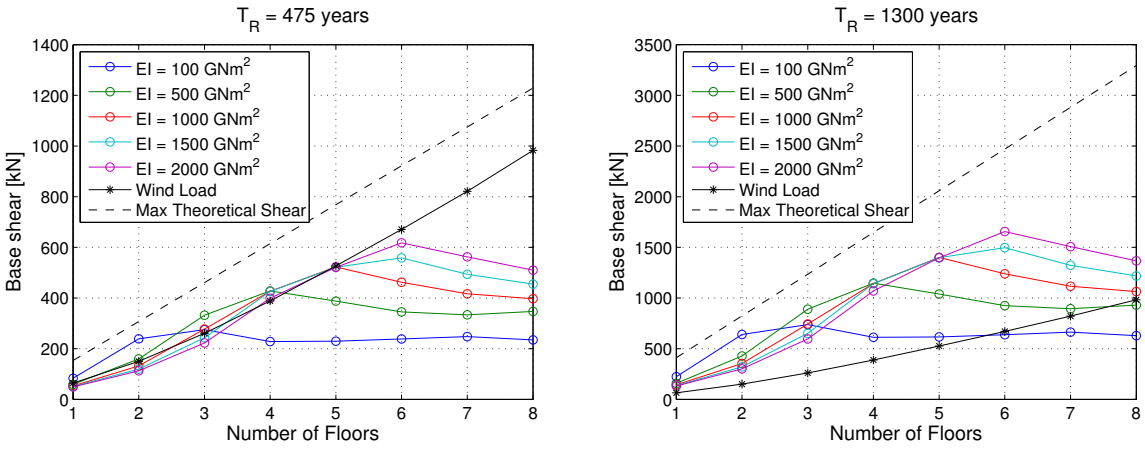

(a) (b)

Figure 33: Cantilever buildings response for T_R =475 (a) and T_R =1300 (b).

As shown in Figure 33(a) an earthquake with a return period of 475 years produce a base shear that envelopes the wind response for a significant amount of cantilever buildings between 1 to 4 floors. The general response is however quite similar or less than the wind response. The buildings that are potentially critical are short, $\leq$ 5 floors, as taller buildings push the first eigen period beyond the constant acceleration branch. It is also

noted that it is difficult to correlate the magnitude of the response with a certain stiffness EI as these tend to overlap each other. The highest seismic/wind response ratio is in fact found for the two story $EI = 100\text{GNm}^2$. At this short height buildings tend to have so high lateral stiffness that the eigen periods go to zero, i.e. the structural acceleration basically follows the ground acceleration. Short buildings with slender elements can however push the spectral ordinates towards peak spectral acceleration. However, it is important to have in mind that these models (cantilever buildings) improve with the stiffness since the slabs are assumed to be slender and the actual stiffness contribution from the slabs becomes less significant with increasing stiffness of the vertical members. Nonetheless, the results from the shear building also suggest short and slender buildings could be critical as the shear building per definition has relatively slender vertical elements.

The 1300-year earthquake envelopes the wind response for almost every single parameter investigated in this study. As seen in Figure 33(b) the seismic response is more than twice as large as the wind response for a good portion of the investigated buildings. It must be assumed that the cantilever buildings are stabilized with shear walls which perhaps is a more reasonable assumption for consequence class IV buildings as well.

5.3 Concluding remarks

The parametric study of the beam models showed that shorter buildings experienced the largest seismic response compared to the wind. For buildings ≤ 2 floors it is likely that a more slender system is the most critical. In theory, this could also be applicable to buildings with a soft story at ground level and a rigid second and/or third floor. An example of a soft story building is a building with an open plan commercial ground floor and the rest of the above stories consists of apartments separated with walls. This system would more or less behave like a SDOF-system when exposed to an earthquake and the majority of the mass would thus be located in the first bending mode, equivalent to a shear building. Stiffness irregularities like this were not explicitly investigated but this conclusion can nonetheless be made since the analysis of the shear building shows that buildings with only one significant mode can reach a base shear proportional to the total mass of the building. Furthermore the largest theoretical base shear could practically be obtained for these buildings if the eigen period is within 0.1 and 0.2 seconds. This means a large amount of mass will be shearing the columns as shown in Figure 34.

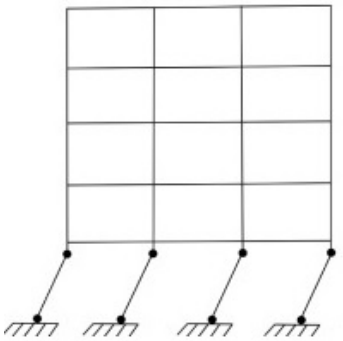

Figure 34: Illustration of a soft story mechanism.

Although the soft story building is an interesting case, the results presented in Section 5.2 should first and foremost be seen as fairly accurate for buildings which have the following properties:

- Symmetry in plan
- Symmetry in elevation

These points are brought up because these buildings were modeled as 2D-beams with constant stiffness EI along the length of the beams. No 3D-effects were investigated whereas it was assumed the earthquake only acted in one direction as it is not possible to investigate orthogonal effects in two dimensional models. Overall, the results can only be seen as accurate for structures where a beam model is feasible. This is certainly not obvious for all structures.

These requirements may seem like excessive idealizations for most buildings. However, in the next section a parametric study of a realistic 3D-model is performed. It will be shown that it is possible to estimate a buildings equivalent beam properties in order to obtain roughly similar response from a 2D beam model and a 3D FE-model, at least if the orthogonal response is small when the building is excited in its main structural directions.

6 Parametric study of realistic 3D FE-model

In addition to the parametric study that was described in Section 5 a parametric study of a 3D FE-model has been performed. This study does not investigate the same range of parameters, instead it has been focused on investigating the influence of various numbers of stories with the same stabilizing system. The analyzed building is modeled according to drawings, showing the stabilizing system, of a 7-story building. The analysis is made using modal response spectrum analysis. In a 3D FE-model it is impossible to include all frequencies of the system. The number of frequencies used is adjusted to fulfill the requirements in Ec8. The requirements according to SS-EN-1998-1 is that the sum of the effective mass for the modes taken into account should at least represent 90 % of the total mass [4].

Parallel to the analysis of the 3D model, a 2D beam model has been analyzed with an approximated stiffness of the 3D model. The purpose is to evaluate the accuracy of the beam models and evaluate the results from the previous parametric study in a more realistic context.

6.1 Model description

The building is rectangular with a width of 16.7 meters and length of 50.4 meters. The hight of each level is 3.5 meters, see Figure 35. For more detailed measurements of the buildings principle plan, see Appendix A.

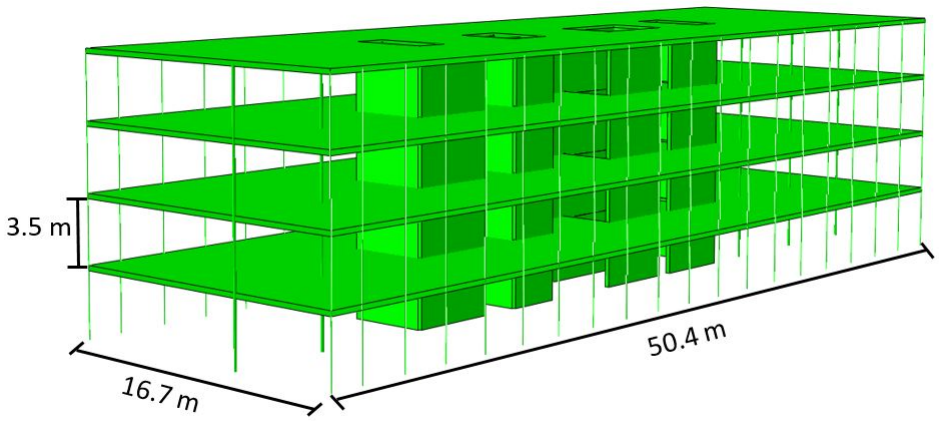

Figure 35: 3D visualization of the models geometry.

The floors consists of 0.265 meters thick concrete hollow core slabs. The columns are made out of steel. The thinner columns along the length of the buildings perimeter are out of type VKR 100x100x10 mm. The inner columns consists of type VKR 400x400x10 mm. The buildings walls are made out of concrete and have a thickness of 250 mm or

150 mm. Detailed description of the walls is presented in Figure 36. Material properties used in the model is found in Table 8.

Table 8: Material properties for the 3D model.

Material	Elastic modulus, E [GPa]	Density, ρ [kg/m^3]
Concrete, walls	35	2400
Concrete, slabs	35	1603[a]
Steel, columns	210	7800

[a]Combined weight of hollow core slab and quasi-permanent live load.

As stated in Table 8 the density of the hollow core slabs include a mass equivalent to the quasi-permanent load. The bulk density of the hollow core slabs is 1320 kg/m^3. The quasi permanent load is calculated with equation 89, according to Eurocode, with Q_k=250 kg/m^2 and ψ_2=0.3.

$$Q_d = Q_k \cdot \psi_2 \tag{89}$$

The calculated load equals 75 kg/m^3 and by dividing it by the height of the hollow core slabs it gives a density of 283 kg/m^3.

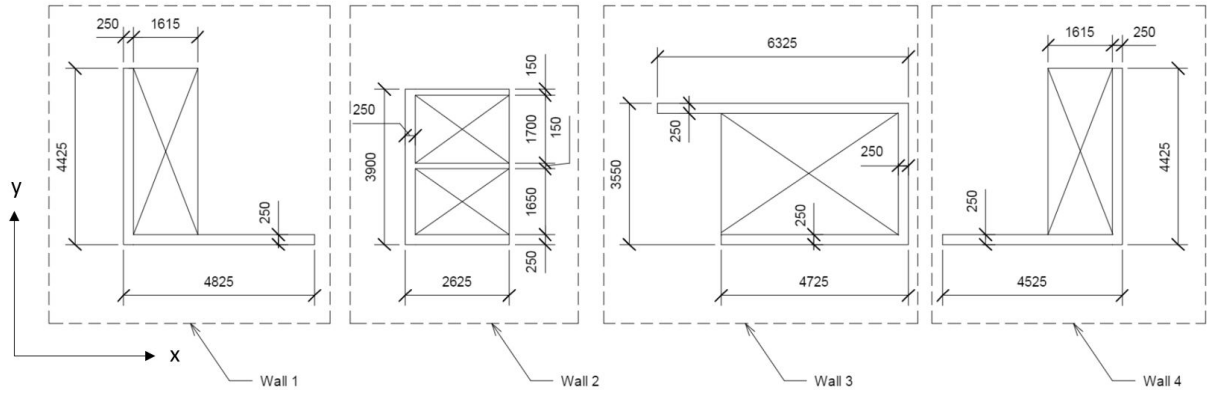

Figure 36: Wall numbering and measurements.

6.1.1 FE-model

The building is modeled with shell elements to represent all surfaces, i.e walls and floors. The connections between the slabs and the walls are prescribed as rigid connections. The thickness of the elements are set according to the described geometry in the section above. The elements used in Abaqus are of type S4R, these are four node shell elements that use reduced integration. The element size of the mesh is approximately 0.4x0.4 m^2. At

ground level all wall nodes are tied to a reference point that is located at the center of the building. The reference point is assigned boundary conditions of no translations and no rotations.

The columns are modeled with truss element, denoted T3D2 in Abaqus. The VKR 100x100x10 and VKR 400x400x10 have a cross section area of 3000 mm^2 and 16000 mm^2 respectively. Each column consists of one element that is connected to the floors as hinges. At ground level the columns are restricted from any translations.

6.1.2 Loads

The type 2 elastic design spectrum according to Eurocode 8 and SHARE parameters was used in this analysis, see Equations 63 to 66. The analysis was only made for importance class IV, i.e. the reference ground acceleration corresponds to a return period of 1300 years. See Figure 18 for complete spectra.

The wind load used in this study is almost the same as described in Section 5.1.4, with the modification according to equation 82. The only difference is that the wind load is applied as a line load at the edge of each floor. The load is calculated for the height of each story and then multiplied with a reference height of 3.5 meters if it is an intermediate floor or 1.25 meters if it is a top floor, see Figure 37. In Table 9 the wind load is presented for each floor. Since the number of floors is varied, floor 4-7 can both act as an intermediate floor or a top floor.

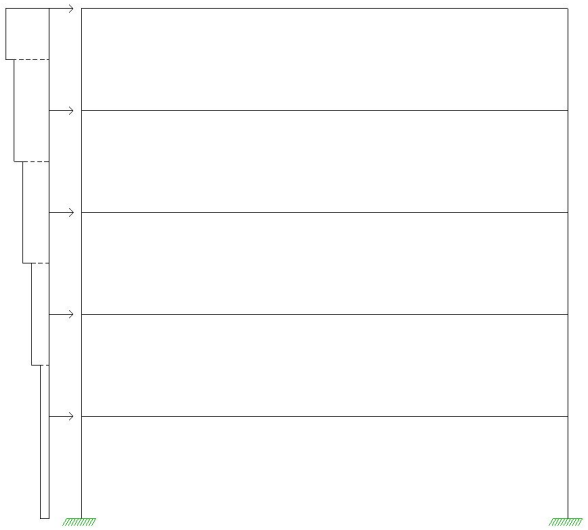

Figure 37: Illustration of the wind load at each floor (not scaled according to magnitude).

Table 9: Wind loads for intermediate floors and top floors.

Level	Load [kN/m]	
	Intermediate floor	Top floor
1	3.34	-
2	3.91	-
3	4.52	-
4	5.05	2.53
5	5.48	2.74
6	5.82	2.91
7	-	2.18

6.1.3 2D Model

Since the building was stabilized through shear walls it was assumed that the cantilever building was the most appropriate 2D-model to use as a comparison. In order to make the two different models comparable the stiffness of the building were estimated. In Table 10 the calculated moment of inertia, for each wall group described in Figure 36, is presented. When the moment of inertia was calculated it was done for each wall group individually and then added together.

Table 10: Wall dimensions and moment of inertia about local x- and y-axis per wall cluster.

Wall number	I_x [m^4]	I_y [m^4]
1	3.96	4.94
2	2.81	1.88
3	2.23	11.8
4	3.89	4.12
Sum:	12.9	22.7

The cantilever model is the same as described in Section 6. The parameters used in the model is presented in Table 11. The mass of the beam is based on the total cross sectional area of all the walls multiplied with the concrete density.

Table 11: Equivalent beam properties.

Parameter	Value
EI_x	450 GNm^2
EI_y	800 GNm^2
m_i	332 000 kg
$\hat{m}$	24 000 kg/m

6.2 Comparison of beam model and 3D FE-model

The total amount of participating mass in the beam model is approximately 100 % for all cases. In the FE-model the participating mass is within a range of 90-96 % for all cases. These values were produced when using 150 eigen frequencies in the RSA. This fulfills the requirement according to Ec8, stated in previous section.

6.2.1 Effective mass

To give a better understanding of the differences between the beam model and the FE-model the results of the accumulated effective mass are presented respectively in Figure 38.

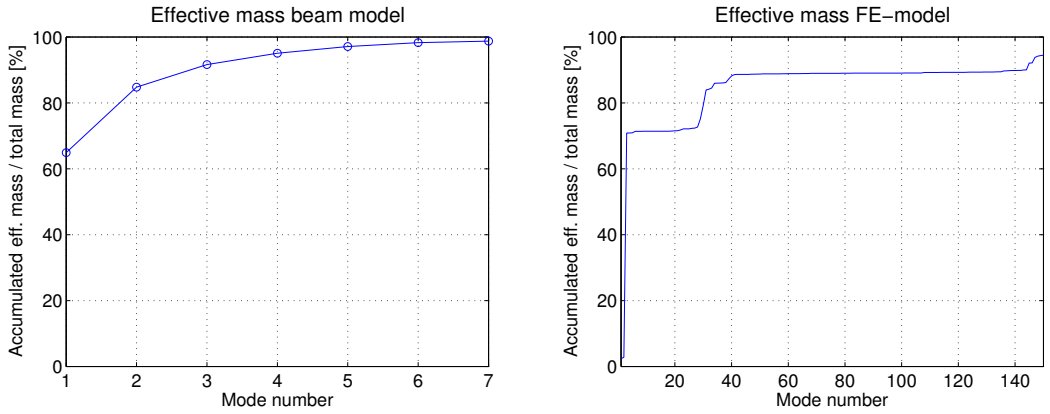

(a) (b)

Figure 38: Accumulated effective mass for a 7 story building excited in the x-direction, Beam model (a), FE-model (b).

The results show that the effective mass is decreasing with the mode number for the beam model. This is not as clear for the FE-model. The steeper sections in Figure 38(b) are modes containing a more significant amount of translation in the excited direction. In some cases even torsional modes contributes to some amount e.g the first mode for a 4 story building, see Table 12 and Figure 39.

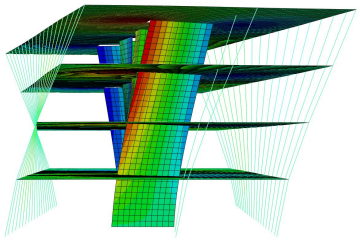

Figure 39: First torsional mode for the 4 story case.

The amount of effective mass is marginal for the main part of the modes in the FE-model. These stagnated areas in Figure 38(b) are modes that contains minor amount of translation or rotations, or they contain mainly translations in the y-direction. This is a significant difference between the models since the beam model only will produce bending modes given in the direction of excitation. As a result the FE-model will better show the structures behavior during an earthquake, at the same time the results get more complex and harder to interpret.

In Table 12 and 13 the effective mass and the associated natural period for each direction of excitation is presented for both models. It is only the first two bending modes and in two cases the first torsional mode that are clearly defined and have more then 3 % effective mass when analyzing the results from the FE-model. In both directions it can be seen that for a lot of the cases modes are split. In general the amount of effective mass within the first mode is almost the same for both models. The only exception is the first mode for a 4 story building excited in the x-direction, see Table 12. This mode is split into two separate parts with a small difference in natural periods. If the effective masses were to be added, it equals 68.3 % witch is in line with the rest of the results.

Table 12: Modes containing more than 3 % effective mass in the in the x-direction.

		Abaqus		Matlab	
Number of floors	Mode	Effective mass x [%]	T [s]	Effective mass x [%]	T [s]
4	1^{st} torsion	3.4	0.293	-	-
	1^{st} bending*	15.6	0.154	-	-
	1^{st} bending	52.7	0.150	67.7	0.16
	2^{nd} bending*	3.1	0.045	-	-
	2^{nd} bending	5.5	0.044	20.6	0.026
5	1^{st} torsion	3.0	0.405	-	-
	1^{st} bending	68.3	0.204	66.4	0.25
	2^{nd} bending	11.3	0.056	20.3	0.039
6	1^{st} bending	68.1	0.262	65.5	0.35
	2^{nd} bending	8.8	0.070	20.0	0.055
	2^{nd} bending*	3.1	0.069	-	-
7	1^{st} bending	68.0	0.324	64.9	0.47
	2^{nd} bending*	4.2	0.086	-	-
	2^{nd} bending	4.6	0.086	19.9	0.074

Table 13: Modes containing more than 3 % effective mass in the in the y-direction.

		Abaqus		Matlab	
Number of floors	Mode	Effective mass y [%]	T [s]	Effective mass y [%]	T [s]
4	1^{st} bending	69.8	0.206	67.7	0.22
	2^{nd} bending	8.7	0.060	20.6	0.035
5	1^{st} bending	67.9	0.287	66.4	0.33
	2^{nd} bending*	4.5	0.081	-	-
	2^{nd} bending	8.8	0.073	20.3	0.052
6	1^{st} bending	66.5	0.381	65.5	0.46
	2^{nd} bending*	3.3	0.103	-	-
	2^{nd} bending	9.5	0.094	20.0	0.074
7	1^{st} bending	65.6	0.488	64.9	0.62
	2^{nd} bending	13.5	0.120	-	-
	2^{nd} bending*	3.7	0.108	19.9	0.10

In Figure 40 the two mode shapes for the split first mode, for the four story building, can be seen respectively.

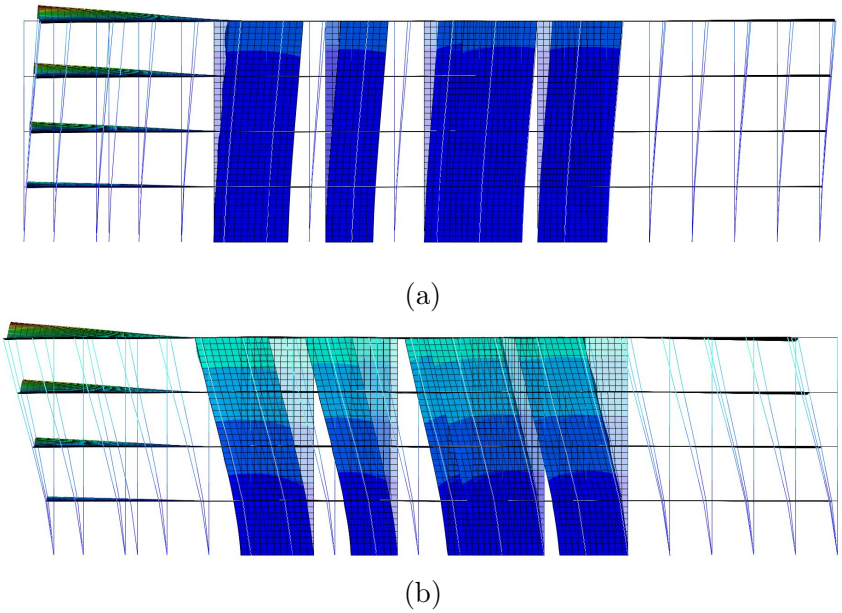

(a)

(b)

Figure 40: First bending mode split into two. Effective mass: (a) = 15.6 % (b) = 52.7%.

This split can have a significant impact when summarizing e.g. the modal contribution when calculating the response. Different modal summation methods will provide different *actual* modal response from this mode. This will be further explained in the next section.

If an absolute summation of the effective mass would to be performed for the split second bending mode for a 7 story building in Table 12, the effective mass presented in the table would add up to 8.8 %. This is because the second mode is divided into multiple modes with less than 3 % effective mass which are not included in the table. In Figure 38(b) the multiple modes containing the different parts of the second bending mode appear between mode 20 and 40. To give a rough estimate of the effective mass content in that region it is approximately 17 %. This can be observed for all split modes, although the content will be found within different mode regions and the approximated amount will vary, still being significantly larger than what is presented in Table 12 and 13.

6.2.2 Comparison of base shear

The estimated maximum response from the modal response analysis are presented in Table 14 and 15. The results presented in the both tables can be found plotted for each direction in Figure 41.

Table 14: Base shear [kN] based on direction of excitation using SRSS as modal summation and combined results (SRSS). Comparison with equivalent beam model in matlab.

	Excitation x		Excitation y		SRSS		Matlab	
Number of floors	Vbx	Vby	Vbx	Vby	Vbx	Vby	Vbx	Vby
4	1283	237	237	1586	1305	1603	1528	1402
5	1960	276	276	1398	1979	1425	1529	1183
6	1835	247	247	1269	1852	1293	1342	1095
7	1733	227	227	1237	1748	1258	1264	1132

Table 15: Base shear [kN] based on direction of excitation using CQC as modal summation and combined results (SRSS). Comparison with equivalent beam model in matlab.

	Excitation x		Excitation y		SRSS		Matlab	
Number of floors	Vbx	Vby	Vbx	Vby	Vbx	Vby	Vbx	Vby
4	1619	241	241	1605	1637	1622	1528	1402
5	1980	268	268	1433	1998	1458	1529	1183
6	1872	243	243	1342	1888	1364	1342	1095
7	1813	221	221	1321	1826	1339	1264	1132

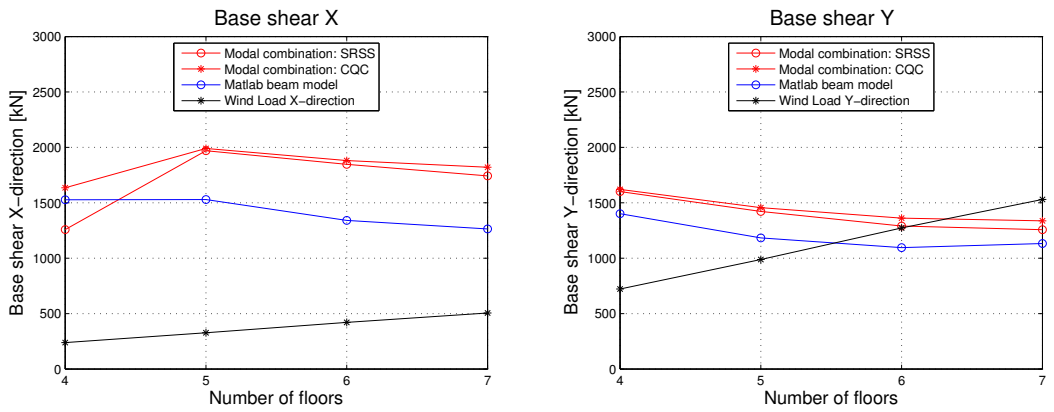

(a) (b)

Figure 41: Base shear comparison. Blue showing base shear for equivalent beam model. Orthogonal response are summed using SRSS in the Abaqus model.

Looking closer at the results in Table 14 and 15 they show that when exciting the model in either the x- or y-direction it gives components of base shear in the orthogonal direction. This orthogonal response indicates that there are possible other directions of excitation that would yield larger response which is why SRSS is used to combine the same response entity from orthogonal excitations. Even though these contribution at first sight could

seem relevant, they have minor impact on the total reaction in each direction for this building. It can be seen in Table 14 and 15 that the combined base shear (SRSS) is not much different, ca 1 % greater, from the base shear components obtained from excitation in the same direction as the component.

The results for the combined directional contributions in Table 15 indicates that the base shear is generally larger in the x-direction. If the natural periods for each direction in Table 12 and 13 are compared it can be seen that the periods are lower for each mode in the x-direction for all cases. This means that the building is stiffer in the x-direction, which correlates to the amount of shear walls in each direction, referring back to Figure 36. Looking at the first mode for each case, which have the greatest impact on the results, their natural periods are located either on or closer to the constant acceleration branch (between 0.1 and 0.2 seconds) in the design spectrum, i.e the results are expected to be greater in the x-direction.

The results for a 4 story building excited in the x-direction differs significantly when using SRSS or CQC as the summation rule for modal combination, see Table 14 respectively 15. As described in Section 2.3.8 : SRSS is a modal combination rule accepted for structures with well separated frequencies. For the 4 story building the first mode is split into two. The two parts have almost the same natural period which means they are practically the same mode and SRSS summation will not accurately sum the modal contributions. The most reasonable summation method for a split mode would arguably be an absolute summation. In Table 16 the result of modal combination for the two parts of the split mode are presented, using different summation methods. The table shows that using absolute sum (ABS) and CQC will give similar results and SRSS summation will result in remarkably lower base shear.

Table 16: Response from the two parts of the first bending mode (4-stories) with different summation methods.

Sum. method:	ABS	CQC	SRSS
Vbx [kN]	1584	1570	1232

Comparing the results presented in Figure 41 the two models behave in a similar manner, although slightly lower response in the matlab beam model. The differences can to a great extent be explained with the wall-slab interaction which was neglected in the beam model. The wall-slab interaction is obvious for bending about the Y-axis since the walls are aligned in the X-direction as seen in Figure 42.

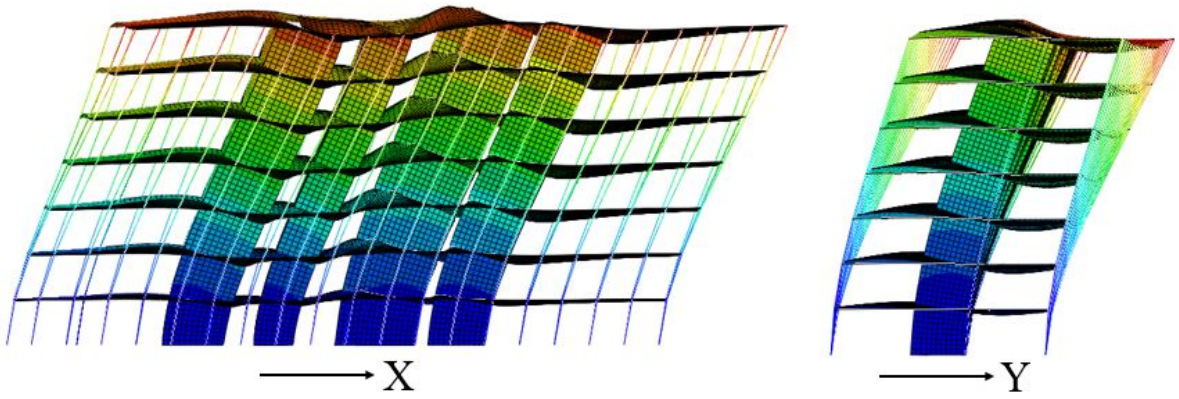

Figure 42: First bending modes. Bending about Y-axis (left) and X-axis (right).

This interaction provides rotational stiffness and since bending about the Y-axis produce a great amount of base shear in the X-direction this response entity is expected to differ more between the FE model and the beam model. In general, it could be seen as the beam model underestimate the response. However, a more correct way to look at it is that the beam model underestimate the stiffness. The mode shapes are quite similar and consequently the effective mass in the first mode is only different with a few percent. Small differences in frequencies can however change the response drastically since these correlates to spectral ordinates in a very steep spectrum. Thus, the investigated parameter EI in the parametric study of the **cantilever building** should be taken with caution as the bending stiffness of a beam and a building does not exactly correlate. However, since a large range of values EI in the previous study were investigated the general observation cannot be altered with; an earthquake with a return period of 1300 years would produce, for most buildings up to 8 stories, more base shear than the wind load.

The wind load creates significantly less base shear than the modal response analysis in the x-direction for both the beam model and the FE-model. In the y-direction the wind still creates less forces for 4- and 5-stories.

6.3 Concluding remarks

The results presented in Section 6.2 shows that the 2D model and the 3D model gives roughly similar results. Even though the complexity of the 3D model is much greater, it could be argued that it shows the same tendencies as the 2D model. Notably is that the wall assembly used, with a slight asymmetric geometry, gave some orthogonal effects. These effects do not significantly affect the results. This suggests that the 2D model can be used for rough estimates for buildings with symmetry in plan end elevation, but also for buildings with a slight asymmetry in plan.

The two studies has so far only measured the differences in base shear. To complement these studies, and give a more detailed description of the earthquake response, sectional forces and moments will be analyzed in the next section.

7 Case study : 5-story building

This case study is an extension of the parametric study that was carried out in the previous section. After analyzing the results from the parametric study it was decided to further analyze a five story building.

The model used is the same as for the parametric study, only now with a constant number of levels. In order to make a more detailed comparison between wind loads and seismic loads, sectional forces and moments in one of the walls will be analyzed. The wall that is to be analyzed is Wall 3, see Figure 36. The three wall segments are assumed to act as one cross section, i.e forces and moments are calculated for the whole cross section. Figure 43 shows the shear center and the centroid of wall 3.

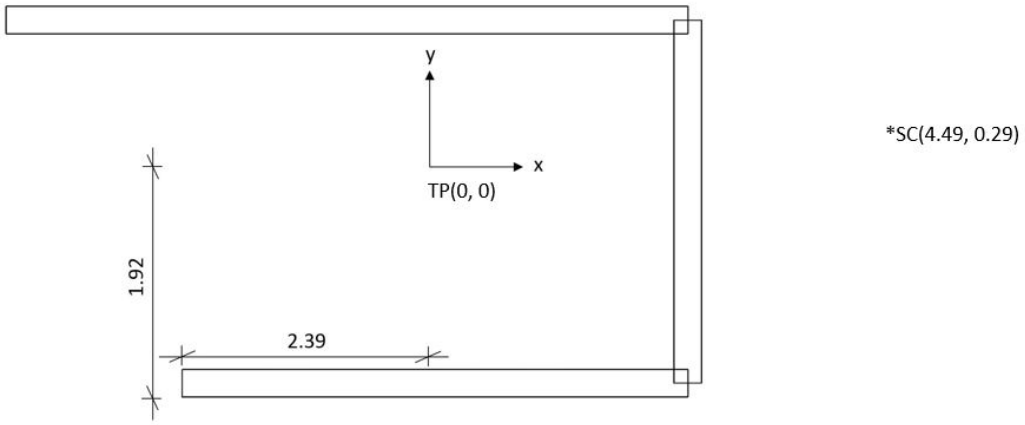

Figure 43: Position of centroid and shear center in Wall 3.

7.1 Analysis

The analysis is made using the first 150 modes in the RSA. This is considered to be sufficient since the effective mass content is more than 90 %, which was concluded in the previous parametric study. Both a 1300 and a 475 year return period based design spectrum was used in the RSA to be compared with wind loads in each direction.

Forces and moments will be calculated at each floor, more specifically for the a row of elements just above and below the floor slabs, see Figure 44.

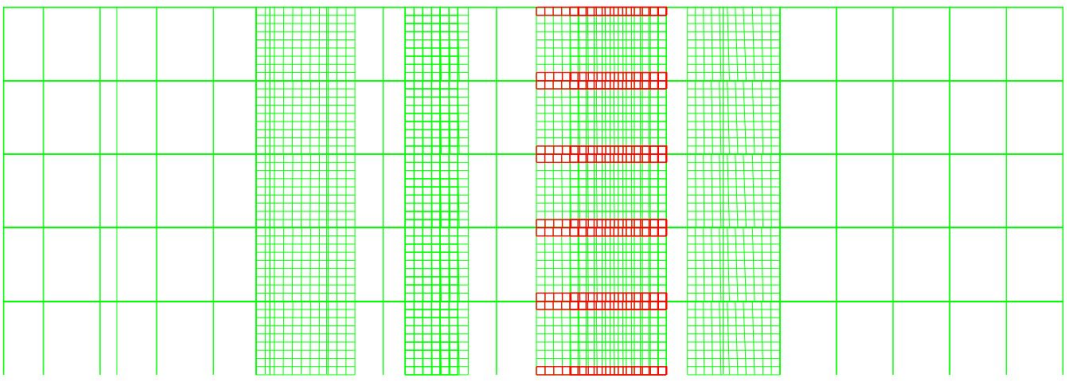

Figure 44: Locations of free body cuts.

By making a horizontal free body cut of the wall, the internal element forces can be integrated and summed, resulting in modal components of section forces and moments. The shear forces and the torsional moment will be summed at the wall's shear center, whereas the bending moments and normal force is summed at the centroid. This was done for each mode, by calculating the element forces produced by the displacements of the mode vectors. These section forces are proportional to the actual modal section forces. Looking at equation 49, repeated here:

$$\boldsymbol{u}_n = \boldsymbol{\phi}_n \Gamma_n \frac{A_n}{\omega_n^2} \tag{90}$$

It can be seen that the mode vector is proportional to the modal displacements with the scale factor $\Gamma_n \frac{A_n}{\omega_n^2}$. The same scale factor can be used when converting the modal components for each mode into contributions of sectional forces and moments.

The procedure to evaluate the section forces from the displacements of the mode shapes and then converting them with a factor $\Gamma_n \frac{A_n}{\omega_n^2}$ is in theory the same procedure that was done in the previous analyzes. However, it was considered important to point out this "detour" as it is incorrect to calculate section forces from modally combined element forces. The section forces have to be calculated for each mode as it is the section forces that are the response entities that should be combined, not the element forces. This was not an issue in the previous analysis as the reaction forces, which were analyzed, were calculated for each mode by default.

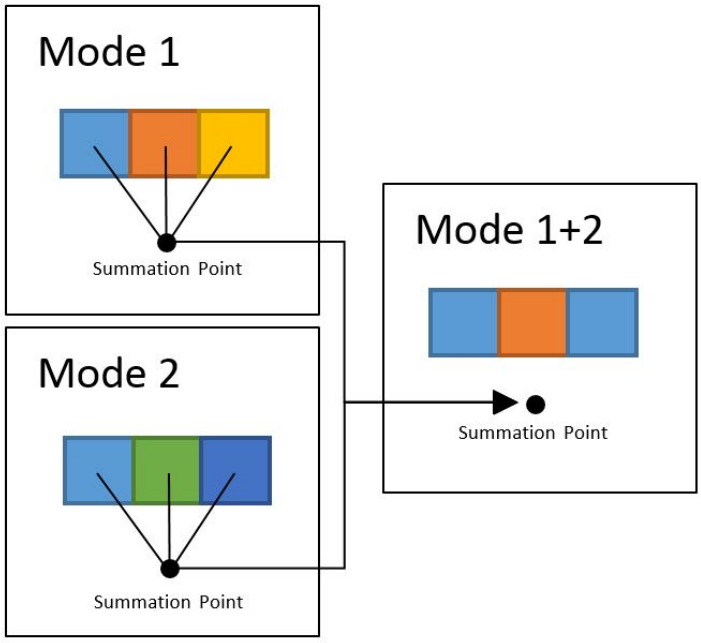

Figure 45: Correct summation path. Combined element forces cannot be integrated to a summation point.

The contributions from each mode were combined using CQC and orthogonal effects were combined using SRSS.

7.2 Results

The total base shear force is presented in Table 17.

Table 17: Enveloped base response [kN].

	$T_R = 475$	$T_R = 1300$	Wind load
Vbx [kN]	748	1998	327
Vby [kN]	546	1458	988

Assume this 5-story building was designed for a total base shear force of approximately 1000 kN due to wind against the long side. This is the largest theoretical base shear in any direction due to wind and it acts in the short direction of the building, see V_{by} in Table 17. If this building is analyzed using the 1300 - year spectrum, the seismic response is $\approx$ 2000 kN in the long direction and $\approx$ 1500 kN in the short direction. As a consequence, the seismic response envelopes the largest wind response, independent of the direction of the earthquake. In fact, the base shear is more than six times greater than that due to wind when analyzing the structure in the long direction.

If the building is analyzed with the 475- years spectrum, the seismic response envelopes the wind in the long direction where it is roughly twice as large. However, the wind remains as the most critical load case when analyzing the base shear in the short direction.

The magnitude of the reaction forces and moments (including components of normal forces and torsion) in each wall is presented in Figure 46.

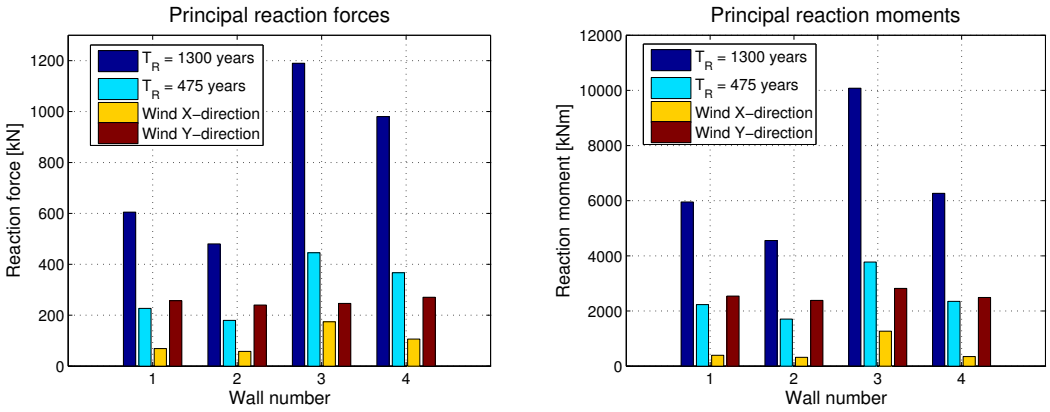

(a) (b)

Figure 46: Resultant forces and moments in each wall at ground level.

Overall the 1300-years earthquake produce reaction forces and moments much greater than the wind load. This was expected due to the large differences in base shear. The distribution of forces and moments suggests that wall 3 is relatively critical due to seismic loading. The seismic response is weighted towards this wall since it has relatively large moment of inertia about the y-axis. Wind against the short side follows the same pattern, however this response is much smaller which is why this wall was interesting to analyze further.

Section forces and moments, evaluated from the free body cuts of wall 3, are presented in Figure 47.

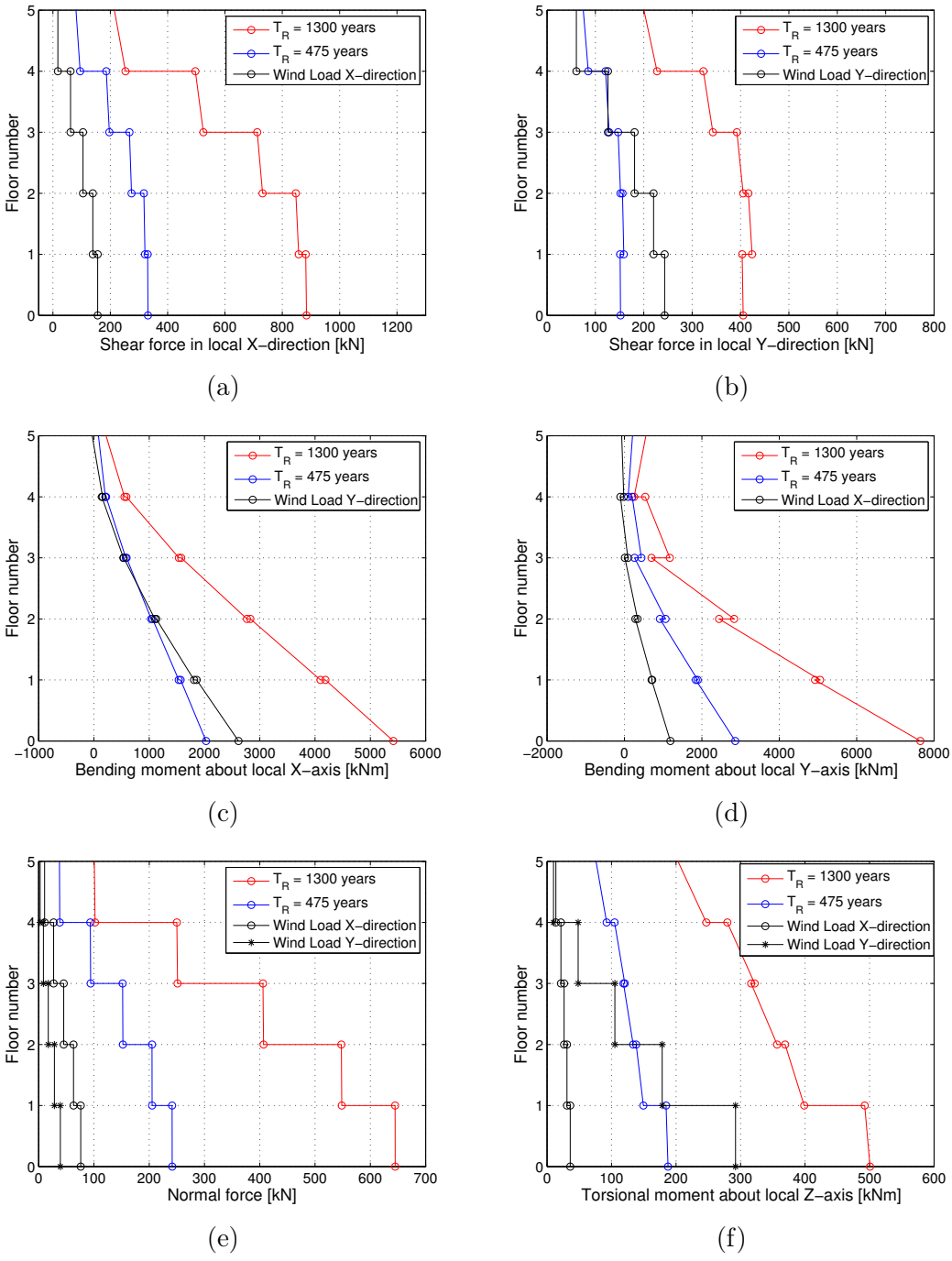

Figure 47: Section forces and moments in wall 3.

- In general the results show that the T_R=1300 years spectrum consistently gives a response greater than the wind load at all floors.
- The shape of the response shows a similar tendency i.e the wind response and the seismic response have similar shape, with the exception of shear force in local

y-direction where the seismic response is marginally larger at the second floor, see Figure 47(b). This is a counter intuitive example where the seismic response deviates from the expected behavior of a cantilever beam in bending.

- When analyzing the results for the T_R =475 years spectrum they show larger response compared to the wind for shear forces in the x-direction and bending moment about the local y-axis. For bending about the x-axis and shear force in the y direction, a tendency of the wind response being larger at the base of the building and at the top, the earthquake response is marginally larger than the wind.
- The plot showing normal forces, Figure 47(e), is mainly presented to show that earthquakes due to horizontal excitement can produce normal forces relatively large compared to the wind. The magnitude of these forces is most likely insignificant when compared to normal forces in this wall produced by the buildings dead weight. However, other structural parts of the building could be more critical.

8 Conclusion

The conclusions presented in this section are drawn from the results of the parametric study where a pair of 2-dimensional beam models were investigated for a large range of stiffness/mass ratios. These parameters were implemented as bending stiffness EI of the beams and number of floors in a 20x20 m^2 building. The results were concluded to be valid for structures with symmetry in-plan and in-elevation. This was confirmed from the parametric study of a 3D-model which showed that the beam models are able to fairly accurate capture the behavior of a realistic 3D-model where the orthogonal response is small. The beam models can estimate the most significant mode shapes and consequently yield an accurate measure of the effective mass for these buildings. However, the beam models either underestimate (cantilever buildings) or overestimate (shear buildings) the stiffness which is why the values of the parameter EI should not be taken literately as the bending stiffness of a building.

This paper is fairly limited to analyzes of total base shear forces. It was however shown in the case study that the base shear is a good indicator of the overall response in a building, when compared to the wind response. The overall seismic response was in general largest at the base in the shear wall that was analyzed. Larger section forces was however found one and two stories up, see Figure 47, which shows that the seismic response is not necessarily largest at base in individual segments of a building. Furthermore, the section forces in this wall was just one selection of response quantities that can be evaluated. The conclusion that can be drawn from this is that the base shear is a non-conservative measure when evaluating the seismic response to the wind response.

The objective was to find buildings with properties that could be considered to be critical to earthquakes in Sweden. The findings in this paper is highly dependent on the target-reliability of the structure, however potentially critical buildings were found in both investigated importance classes II and IV, each presented in Section 8.1 and 8.2.

8.1 Buildings of ordinary importance

Looking closer at the result from the first parametric study presented in Figure 33 it was only a few buildings that exceeded the response from the wind load. As a reminder, the plot shows the response for a quadratic building. If the same analysis was made with a rectangular building similar to the one used in the case study, the results would show a greater range of buildings exceeding the wind response. This can be explained by the size effect described in section 5.1.2. The size effect is quite relevant for elongated buildings, as most of the horizontal capacity in general are engineered for wind against the long side. The case study is an example that shows how the seismic response envelopes the wind for response quantities related to wind against the short side.

The case study showed that both shear forces in the long direction and bending moment acting in the long direction exceeded the wind load response when analyzed using the

475-year spectrum. In relation to these results it is important to consider what type of buildings is correlated to importance class II. Apartment buildings is an example of buildings belonging in this category, see Table 1. When designing such a building there are codes, regulating e.g. fire safety, that will require each apartment being separated as their own fire cell. A way of solving this is with the use of concrete walls as separating elements between apartments. This type of solution leads to a larger amount of shear walls in the buildings, which could make the capacity to handle horizontal loads much greater than forces and moments produced from any horizontal action. This suggest that the findings are not necessarily as critical as they might seem for the 475-year spectrum. It is however obvious that the seismic load could be the designing load case, if only compared to the wind, especially in the long direction of elongated buildings.

8.2 Buildings of vital importance

Buildings of vital importance correlates to importance class IV and these were analyzed for an earthquake with a return period of 1300 years. It is important to point out that this return period is not mentioned in Eurocode 8. It was concluded that using a recommended importance factor $\gamma_I = 1.4$ in order to differentiate buildings of vital importance yielded "actual" return periods depending on seismicity at site. Sweden and other low seismicity areas have a stronger increase in intensity of ground motions with increasing return periods. Thus it was decided to instead choose a ground motion corresponding to a return period derived from recommended parameters in Eurocode since UHS for various return periods are provided through ESHM13.

The base shear due to seismic loading enveloped the wind response for an overwhelming amount of buildings in this category. The seismic response is often more than twice as high for the investigated 20x20 m^2 buildings. It's easier to point out properties of buildings in this category that are not critical to seismic loading; exceptionally slender and tall buildings. Most buildings up to 8 floors (equivalent to 28 meters tall) would produce a larger base shear due to a 1300-year earthquake than that due to wind.

The case study of the 5 story building is an example of a rectangular building that would be considered to be exceptionally critical to earthquake's if designed as a importance class IV building. Not even a very conservative approach, to engineer the same wind capacity in the long direction as in the short direction would be sufficient as the seismic base shear enveloped the wind, independent of wind direction and direction of earthquake. The same goes for any base response that was analyzed in one of the walls. In conclusion, it is obvious that the seismic action in Sweden should not be neglected if Sweden wants to accomplish the same reliability of structures, that are vital for civil protection during an earthquake, as the rest of Europe.

9 Final remarks

In this paper, the seismic response was compared to the wind response as if the wind response somehow represented the horizontal capacity of buildings in Sweden. This topic is discussed through out the paper and this assumption is of course not necessary true. Even so, the wind load is a relevant measure as it is in fact the designing load case for horizontal stabilization in most cases, although design for other accidental loads could provide over all larger horizontal stability.

As the wind load in Sweden is a "default load case" for designers to deal with, there is no reason to neglect the seismic load, as this paper shows, it quite easily could envelope the wind response.

It is easy to mistake the 475 year and 1300 year return periods as too conservative if compared to the return periods of variable actions, i.e. 50 years. The characteristic value of variable actions such as wind actions are expected to occur during the design working life. The seismic action on the other hand could be treated as an accidental action and is unlikely to occur. As a consequence these actions are treated differently in design situations regarding partial coefficients and load combination factors whereas the characteristic values of the variables are designed with a larger degree of conservatism. This was taken into account by designing the wind action as a variable action in the ULS. Furthermore the designing wind action was multiplied with a factor 1.5/1.2 in order to take differences in conservatism on the capacity for variable loads and accidental loads into account. In total, the wind action was $1.5 \cdot 1.5/1.2 = 1.875$ times larger than its characteristic value determined by the return period 50 years. The seismic action on the other hand is exactly equal to the value corresponding to a given return period.

This topic is beyond the scope of structural dynamics, in which the focus of this paper have been made. It is however a most significant topic as the seismic action is greatly dependent on the return period. The authors of this paper can only emphasize that these hazard levels are derived from the current European standard: 475 years are explicitly recommended for structures of normal importance and 1300 years are implicitly recommended for structures of vital importance.

References

[1] J. Woessner, D. Laurentiu, D. Giardini, H. Crowley, F. Cotton, G. Grünthal, G. Valensise, R. Arvidsson, R. Basili, M. B. Demircioglu, *et al.*, "The 2013 european seismic hazard model: key components and results," *Bulletin of Earthquake Engineering*, vol. 13, no. 12, pp. 3553–3596, 2015.

[2] "D1.1 - description of work (dow version 02.04.2012)," in *ENV.2008.1.3.1.1 Development of a common methodology and tools to evaluate earthquake hazard in Europe*.

[3] A. Costa, E. Coelho, A. Carvalho, G. Weatherill, R. Pinho, and H. Crowley, "D2.1-hazard output specifications requirement document, jointly approved with ec8 committee," in *ENV.2008.1.3.1.1 Development of a common methodology and tools to evaluate earthquake hazard in Europe*, 2010.

[4] "Eurocode 8: Design of structures for earthquake resistance-part 1: General rules, seismic actions and rules for buildings," 2004.

[5] B. G. S. ©NERC, "Probalistic seismic hazard assessment," 2013.

[6] "Eurocode 1: Action on structures -part 1-4: General actions -wind actions," 2008.

[7] E. F. for Earthquake Hazard and R. ©ETH Zurich, "Share preferred mean hazard model," 2017.

[8] A. Chopra, *Dynamics of Structures: Theory and Applications to Earthquake Engineering*. Civil Engineering and Engineering Mechanics Series, Prentice Hall, 2012.

[9] J. W. Baker, "An introduction to probabilistic seismic hazard analysis," *White Pap*, vol. 2, no. 1, p. 79, 2013.

[10] P. Bisch, E. Carvalho, H. Degee, P. Fajfar, M. Fardis, P. Franchin, M. Kreslin, A. Pecker, P. Pinto, A. Plumier, *et al.*, "Eurocode 8: seismic design of buildings worked examples," *Luxembourg: Publications Office of the European Union*, 2012.

[11] G. Weatherill, L. Danciu, and H. Crowley, "Future directions for seismic input in european design codes in the context of the seismic hazard harmonisation in europe (share) project," in *Vienna conference on earthquake engineering and structural dynamics*, pp. 28–30, 2013.

[12] G. Weatherill, R. Pinho, and H. Crowley, "D2.2-report on seismic hazard definitioons needed for structural design applications," in *Vienna conference on earthquake engineering and structural dynamics*, pp. 28–30, 210.

[13] "Eurokode 8 - prosjektering av konstruksjoner for seismisk påvirkning, samling av nasjonale tillegg (na)," 2014.

[14] E. Faccioli, M. Fardis, A. Elnashai, and E. Carvalho, "Designers guide to en 1998-1 and 1998-5," Eurocode, 2005.

A Blue print

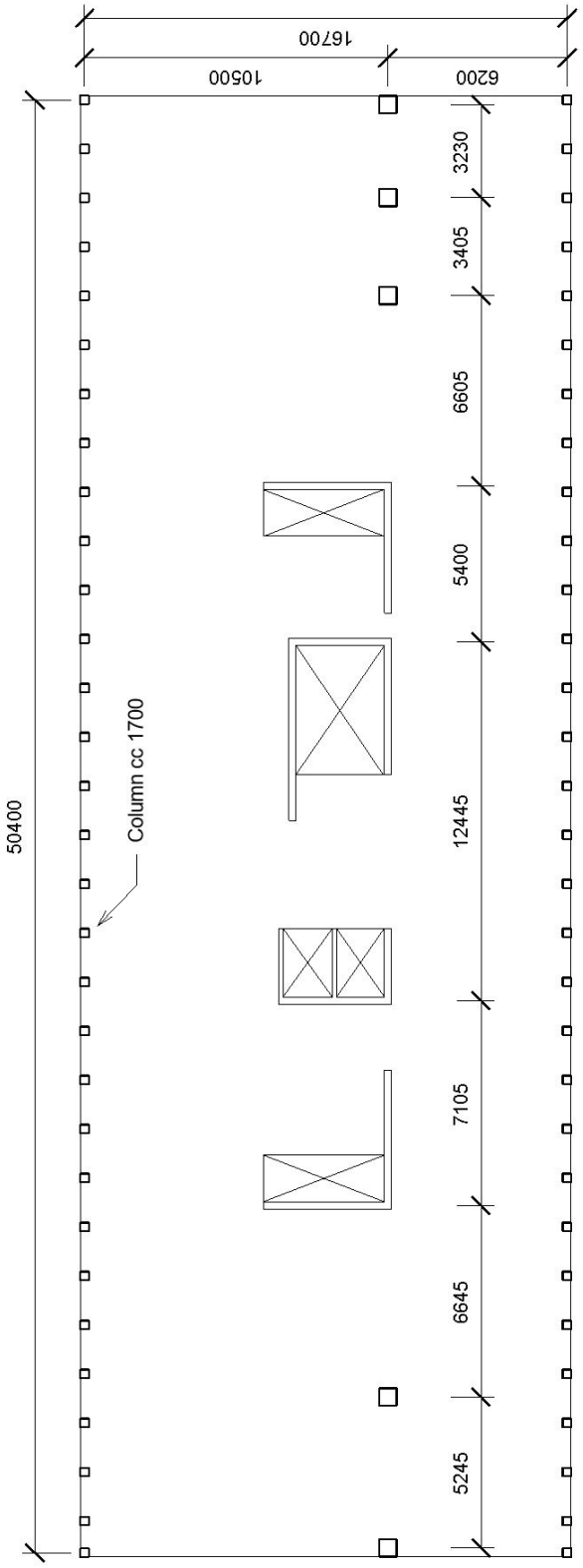
16700
10500
6200
3230
3405
6605
5400
12445
7105
6645
5245
50400
Column cc 1700